Eur. Phys. J. Plus (2025) 140:365
https://doi.org/10.1140/epjp/s13360-025-06300-5

THE EUROPEAN PHYSICAL JOURNAL PLUS

Regular Article

A novel time-delayed stochastic epidemic modeling approach incorporating Crowley–Martin incidence and nonlinear holling type II treatment rate

Abdeldjalil Kadri[1], **Ahmed Boudaoui**[1], **Seham M. Al-Mekhlafi**[2,3], **Saif Ullah**[4,a], **Mohammed Asiri**[5], **Muhammad Bilal Riaz**[6,7]

[1] Laboratory of Mathematics Modeling and Applications (LaMMA), University of Adrar, 01000 Adrar, Algeria
[2] Department of Mathematics, Faculty of Education, Sana'a University, Sanaa, Yemen
[3] Jadara University Research Center, Jadara University, Irbid, Jordan
[4] Department of Mathematics, University of Peshawar, Peshawar, Khyber Pakhtunkhwa, Pakistan
[5] Department of Clinical Laboratory Sciences, College of Applied Medical Sciences, King Khalid University, Abha, Saudi Arabia
[6] IT4Innovations, VSB–Technical University of Ostrava, Ostrava, Czech Republic
[7] Applied Science Research Center, Applied Science Private University, Amman, Jordan

Received: 16 October 2024 / Accepted: 4 April 2025

Abstract Mathematical modeling of infectious disease is essential for understanding the impact of various epidemiological factors and stochastic influences on disease spread. In this study, we investigate a stochastic compartmental epidemic model with time delays, featuring a Crowley–Martin (C-M) incidence rate alongside a holling type II (HT-II) treatment rate. Initially, we demonstrate the existence and uniqueness of a positive global solution to the model. Subsequently, we establish sufficient conditions that lead to the extinction of the disease. A suitability constructed Lyapunov function is used to confirm the presence of a stationary distribution (SD). In epidemiology, the presence of a stationary distribution indicates that the disease will persist over the long term. Additionally, the Fokker–Planck equation is solved to obtain the exact analytical form of the probability density function (PDF) that describes the behavior of the stochastic model near its unique endemic quasi-equilibrium. In statistical analysis, the explicit density function can capture and represent all the dynamical features of an epidemic model. Finally, a comprehensive simulation is provided to support and illustrate our theoretical results, offering practical insights into the model's behavior. This work contributes to the development of more accurate predictive models that can assist public health policymakers in designing effective disease control strategies and intervention plans to mitigate the spread of infectious diseases.

1 Introduction

Epidemic modeling is a crucial tool for understanding the transmission and effective control strategies of infectious diseases [1, 2]. The basic susceptible-infected-recovered (*SIR*) compartmental model, based on three population classes, was initially presented by Kermack and McKendrick in 1927 [3] and remains one of the foundational models for analyzing disease transmission. The fundamental *SIR* compartmental models have been widely formulated and serve as the foundation for numerous extensions, allowing to capture the complexities of real-world disease dynamics and to simulate various epidemic outbreaks with high accuracy [4–6].

Recently, a vast literature has been developed on the extensions of the basic *SIR* transmission model and rigorously studied to better capture the complexities of disease dynamics and their intervention strategies [7–9]. These studies are helpful for understanding the disease spread, as they provide more sophisticated tools for simulating reported outbreaks and evaluating intervention measures [10]. However, among these extensions, most have traditionally been formulated using classical differential equations, which assume deterministic behavior and often overlook critical aspects such as memory effects, time delays, and stochasticity found in various epidemics [11]. To capture a more realistic analysis of real-world epidemics, it is crustal to formulate mathematical models that incorporate both time delays and stochastic phenomena as can be found in [12]. These models are more capable of reflecting the unpredictable nature of an epidemic outbreak and the influence of various external factors. For instance, the incubation period between initial infection and the onset of infectiousness as well as the time needed for treatment and recovery can be accurately described using models with time delays. These delays play a pivotal role in shaping the progression of an epidemic and the timing of control strategies for the infection incidence. In addition to this, stochastic effects capture the inherent randomness and uncertainties associated with disease transmission, such as variations in contact rates, environmental factors, and individual immune responses. Mathematical models based on stochastic differential systems allow for a more realistic representation of epidemics with real-word scenarios specifically, where the outcomes are not purely deterministic but subject to fluctuations influencing the control and spread

[a] e-mail: saifullah.maths@uop.edu.pk (corresponding author)

Published online: 06 May 2025

of infection. These considerations are crucial for developing more precise predictions and for designing optimal control measures [13].

In epidemic modeling with classical differential systems, the treatment rate often considered to be either a fixed value or directly proportional to the cumulative infected individuals in the community. Although, this assumption simplifies mathematical analysis but it fails to account for the real-world constraints on healthcare systems, where treatment resources such as medical staff, hospital beds, and medications are often limited. In a real sense, as the number of infected people increases, healthcare facilities may experience shortages of resource, causing delays or restrictions in treatment availability to the patients. Ignoring these drawbacks can lead to inaccurate predictions of disease spread and ineffective public health interventions. Consequently, it is important to adopt a more realistic modeling approach that accurately represents specific conditions, accounts for resource constraints, and considers the adaptive capacity of healthcare systems. To address these limitations, Wang et al. [14] explored a *SIR* epidemic model in which the treatment rate is assumed to be constant, regardless of the number of infectious people. The treatment rate function of this type is expressed by the following equation

$$\mathcal{H}(I) = b, \quad \text{for } I > 0, \quad \text{and} \quad \mathcal{H}(I) = 0, \quad \text{for } I = 0,$$

where b denotes a constant treatment rate. This assumption ensures that the available medical resources are either unlimited or externally controlled, meaning that treatment is provided at a steady rate, independent of outbreak severity, or healthcare capacity. This type of treatment rate function may be useful in theoretical studies, but it does not adequately capture the impact of resource limitations that often arise during large-scale outbreaks. Keeping this shortcoming in mind, Zhang et al. [15] studied a more realistic treatment function approach incorporating the nonlinearity relation between treatment availability and the number of infected cases. They introduced the following continuously differentiable C^1 function in their model:

$$\mathcal{H}(I) = \frac{aI}{1+bI}, \quad a, b \geq 0.$$

In the above function, the fraction $\frac{a}{b}$ accounts the maximum treatment capacity that can be provided within a given time period. This function, also called as the `HT-II` treatment rate, represents the saturation of medical resources as infection levels rise in a region. Unlike the constant treatment rate assumption, which suggests unlimited treatment availability, the `HT-II` rate function reflects the nature that treatment rate initially increases with the number of infected individuals but eventually plateau when medical resources reach their available limit. The modified nonlinear rate function accurately represents the challenges faced by healthcare officials during an epidemic outbreak, particularly in resource-constrained environments. Moreover, the `HT-II` treatment and incidence rate functions have been applied in other epidemiological models to study diseases with limited medical resources. In [4], researchers utilized the `HT-II` rate function to analyze the dynamical features of a vector-host disease model under constrained treatment scenarios. Their findings indicate that incorporating nonlinear treatment and incidence rate function provide more and epidemiologically feasible outputs into a disease transmission and control. Keeping in mind the situations with the limitations of medical resources, these models offer more accurate predictions of outbreak progression and enable to develop more effective public health interventions.

The function describing infection incidence in an epidemic model is a essential component representing the rate at which the susceptible individuals become infected. Many classical models rely on the bilinear incidence rate of the form ζSI, where ζ is the transmission coefficient [16, 17]. The bilinear rate function fails to capture the complexities of real-world transmission dynamics of an infection outbreak. The primary limitation of the bilinear incidence rate function is its failure to capture the saturation effects which occur when the rate of newly infections does not continue to increase indefinitely as the number of infectious individuals rises. This phenomenon arises due to various factors such as limited contact opportunities, changes in individual behavior in response to the epidemic, and constraints on healthcare resources. To address these limitations, authors have presented various nonlinear incidence functions that establish a better and accurate representation of infection transmission dynamics [18–21].

Crowley and Martin introduced the following generalized form of the functional response in [22]:

$$\mathcal{G}(S,\, I) = \frac{\gamma S(t)I(t)}{(1+\alpha_2 I(t))(1+\alpha_1 S(t))}, \quad \alpha_1, \alpha_2 \geq 0.$$

In this formulation, the authors incorporate saturation effects by reflecting the limitations in contact opportunities and behavioral adaptations during an epidemic outbreak [23]. The parameters α_1 and α_2 control the saturation degree ensuring that as the number of susceptible or infected individuals grows, the rate of new infections does not increase indefinitely. This is particularly important in realistic case scenarios where factors such as immune responses, public health interventions, and social distancing influence the spread of disease incidence. This approach offers a more realistic representation of diseases such as COVID-19, TB, and HIV where resource constraints and behavioral changes significantly influence transmission dynamics.

In [24], Wen et al. discussed the subsequent delayed epidemiological compartmental model with bilinear incidence rate

$$\begin{aligned} S'(t) &= -\gamma I(t)S(t) + \Lambda - \upsilon_S S(t) + \delta e^{-\upsilon_R \iota} I(t-\iota), \\ I'(t) &= \gamma I(t)S(t) - (\upsilon_I + \delta)I(t), \\ R'(t) &= -\upsilon_R R(t) + \delta(I(t) - e^{-\upsilon_R \iota} I(t-\iota)). \end{aligned} \tag{1}$$

In [25], a generalization of model (1) with a saturation incidence rate was proposed. The generalized model is summarized in the following system

$$\begin{aligned} S'(t) &= -\frac{\gamma S(t)I(t)}{(1+\alpha_2 I(t))} - \upsilon_S S(t) + \Lambda + \delta e^{-\upsilon_R \iota} I(t-\iota), \\ I'(t) &= -(\upsilon_I + \delta)I(t) + \frac{\gamma I(t)S(t)}{(1+\alpha_2 I(t))}, \\ R'(t) &= -\delta e^{-\upsilon_R \iota} I(t-\iota) - \upsilon_R R(t) + \delta I(t), \end{aligned} \tag{2}$$

where $S(t)$, $R(t)$, and $I(t)$ denote the number of individuals in the population who are susceptible, recovered, and infected, respectively. Additionally, γ is the contact, Λ is the birth rate, δ is the recovery rate from infection, υ_S, υ_I, and υ_R are the natural death rates of the susceptible, infected, and recovered populations, respectively. In [26], the term $\delta e^{-\upsilon_R \iota} I(t-\iota)$ was introduced, representing individuals who have survived natural death in the recovery pool and become susceptible again, where ι denotes the duration of immunity.

Furthermore, in [5], the following stochastic model was investigated:

$$\begin{aligned} dS(t) &= \Big[-\frac{\gamma S(t)I(t)}{(1+\alpha_2 I(t))} - \upsilon_S S(t) + \Lambda + \delta_0 e^{-\upsilon_R \iota} I(t-\iota) \Big] dt - \eta_1 S(t) dW_1(t) - \frac{\eta_4 SI}{1+\alpha_2 I(t)} dW_4, \\ dI(t) &= \Big[-(\upsilon_I + \delta)I(t) + \frac{\gamma S(t)I(t)}{(1+\alpha_2 I(t))} \Big] dt - \eta_2 I(t) dW_2(t) + \frac{\eta_4 SI}{1+\alpha_2 I(t)} dW_4, \\ dR(t) &= \Big[-\delta_0 e^{-\upsilon_R \iota} I(t-\iota) - \upsilon_R R(t) + \delta I(t) \Big] dt - \eta_3 R(t) dW_3(t), \end{aligned} \tag{3}$$

where η_j and $W_j(t)$, $(j = 1, 2, 3, 4)$ represent the white noise intensity and the independently Brownian motion, respectively, over a complete probability space.

2 Main problem

Motivated by the work studied in [24, 25], and [5], we formulated a more general epidemic model by incorporating the Crowley–Martin incidence function and the holling type II treatment function. In addition, the condition $\delta \geq \delta_0$ is consider in problem formulation.

$$\begin{aligned} dS(t) &= \Big[-\frac{\gamma I(t)S(t)}{(1+\alpha_1 S(t))(1+\alpha_2 I(t))} + \Lambda - \upsilon S(t) + \delta_0 e^{-\upsilon \iota} I(t-\iota) \Big] dt + \eta_1 S(t) dW_1(t), \\ dI(t) &= \Big[-(\upsilon + \delta + \lambda)I(t) + \frac{\gamma S(t)I(t)}{(1+\alpha_1 S(t))(1+\alpha_2 I(t))} - \frac{aI(t)}{1+bI(t)} \Big] dt + \eta_2 I(t) dW_2(t), \\ dR(t) &= \Big[-\upsilon R(t) + \frac{aI(t)}{1+bI(t)} + \delta I(t) - \delta_0 e^{-\upsilon \iota} I(t-\iota) \Big] dt + \eta_3 R(t) dW_3(t), \end{aligned} \tag{4}$$

where λ and υ represent the mortality rates due to the disease and natural causes, respectively. The rest of the parameters are as mentioned above. If $\eta_1 = \eta_2 = \eta_3 = 0$, we recover the deterministic case of the above model.

In the remainder of this work, we first demonstrate the uniqueness and existence of the positive global solution. Sufficient conditions for the disease's extinction are presented in the next section, which is essential for understanding the long-term behavior of the epidemic. Additionally, we construct a suitable Lyapunov function to prove the existence of a SD, providing insights into the long-term behavior of the stochastic system. Finally, the theoretical findings are illustrated by numerical simulations, which serve to confirm the results.

In the onward study, we consider a complete probability space denoted as $(\Omega, \mathcal{F}, \{\mathcal{F}_t\}_{t\geq 0}, \mathbb{P})$, where $\{\mathcal{F}_t\}_{t\geq 0}$ adheres to the standard conditions.

2.1 Existence and uniqueness of global positive solution

We proceed with the following theorem to obtain the desire results

Theorem 1 *For any* $(S(0),\ I(0),\ R(0)) \in \mathbb{R}^3_+$ *with* $S(r) \geq 0,\ I(r) \geq 0$, *and* $R(r) \geq 0$ *for all* $r \in [-\iota,\ 0[$, *the model (4) has a unique positive solution (S(t), I(t), R(t)). Additionally, the solution remains in* $\mathbb{R}^3_+$ *with probability one, which means that* $(S(t),\ I(t),\ R(t)) \in \mathbb{R}^3_+\ \forall t \geq 0$ *almost surely (a.s).*

Proof Coefficients of the model are locally Lipshitz for all $(S(0),\ I(0),\ R(0)) \in \mathbb{R}^3_+$ with $S(r) \geq 0,\ I(r) \geq 0$ and $R(r) \geq 0$, $\forall r \in [-\iota,\ 0[$, we can find a unique solution shown by the set $(S(t), I(t), R(t))$ on $t \in [-\iota,\ \iota_e)$, where ι_e is the explosion time.

We show that the solution is global, i.e., to validate $\iota_e = \infty\ a.s$. Assume that we have a sufficiently large nonnegative number τ such that $S(0), I(0), R(0)$ and $S(r), I(r), R(r)$ all in $[\frac{1}{\tau},\ \tau]$. Let us defining the stopping time as follows

$$\iota_\Gamma = \inf\left\{t \in [0,\ \iota_e) : \min\left\{S(t),\ I(t),\ R(t)\right\} \leq \frac{1}{\Gamma},\ \text{or}\ \max\left\{S(t),\ I(t),\ R(t)\right\} \geq \Gamma\right\}\ \forall \Gamma \geq \tau.$$

We set $\inf \varnothing = \infty$, where $\varnothing$ used for empty set. Clearly, ι_Γ is increasing as $\Gamma \to \infty$. Let

$\iota_\infty = \lim_{\Gamma\to\infty} \iota_\Gamma$, with $\iota_e \geq \iota_\infty\ a.s$. Now we are going to prove that $\iota_\infty = \infty$, the proof goes by contradiction. We assume that $\iota_\infty < \infty$, then exists $T > 0$ and $\varepsilon \in (0,\ 1)$ where $\mathbb{P}\{\iota_\infty \leq T\} \geq \varepsilon$. Therefore, there exists an integer $\Gamma_1 \geq \tau$ so that

$$\mathbb{P}\{\iota_\Gamma \leq T\} \geq \varepsilon, \forall \Gamma \geq \Gamma_1. \tag{5}$$

We consider a C^2-function $\aleph : \mathbb{R}^3_+ \to \mathbb{R}_+$ defined as follows:

$$\aleph(S,\ I,\ R) = S + R + I - 3 - (\ln S + \ln I + \ln R).$$

The nonnegativity of $\aleph$ can be seen from $\nu - 1 - \ln \nu \geq 0, \forall \nu > 0$. Applying the Itô formula, we get

$$\begin{aligned}
d\aleph(S,\ I,\ R) =& \left(1 - \frac{1}{I}\right)dI + \left(1 - \frac{1}{S}\right)dS + \left(1 - \frac{1}{R}\right)dR + \frac{1}{2S^2}(dS)^2 + \frac{1}{2I^2}(dI)^2 + \frac{1}{2R^2}(dR)^2 \\
=& \left(1 - \frac{1}{S}\right)\left(\left[\Lambda - \frac{\gamma I(t)S(t)}{(1+\alpha_1 S(t))(1+\alpha_2 I(t))} - \upsilon S(t) + \delta_0 e^{-\upsilon\iota} I(t)\right]dt + \eta_1 S(t) dW_1(t)\right) \\
&+ \frac{1}{2S^2}\left(\left[\Lambda - \frac{\gamma I(t)S(t)}{(1+\alpha_1 S(t))(1+\alpha_2 I(t))} - \upsilon S(t) + \delta_0 e^{-\upsilon\iota} I(t-\iota)\right]dt + \eta_1 S(t) dW_1(t)\right)^2 \\
&+ \left(1 - \frac{1}{I}\right)\left(\left[\frac{\gamma S(t)I(t)}{(1+\alpha_1 S(t))(1+\alpha_2 I(t))} - \frac{aI(t)}{1+bI(t)} - (\delta + \upsilon + \lambda)I(t)\right]dt + \eta_2 I(t) dW_2(t)\right) \\
&+ \frac{1}{2I^2}\left(\left[\frac{\gamma S(t)I(t)}{(1+\alpha S(t))(1+\sigma I(t))} - \frac{aI}{1+bI} - (\delta + \upsilon + \lambda)I(t)\right]dt + \eta_2 I(t) dW_2(t)\right)^2 \\
&+ \left(1 - \frac{1}{R}\right)\left(\left[\frac{aI}{1+bI} - \upsilon R(t) + \delta I(t) - \delta_0 e^{-\upsilon\iota} I(t-\iota)\right]dt + \eta_3 R(t) dW_3(t)\right) \\
&+ \frac{1}{2R^2}\left(\left[\frac{aI}{1+bI} - \upsilon R(t) + \delta I(t) - \delta_0 e^{-\upsilon\iota} I(t-\iota)\right]dt + \eta_3 R(t) dW_3(t)\right)^2 \\
=& L\Sigma(S,\ I,\ R)dt + \eta_1(S(t) - 1)dW_1(t) + \eta_2(I(t) - 1)dW_2(t) + \eta_3(R(t) - 1)dW_3(t),
\end{aligned}$$

where $L\aleph :\ \mathbb{R}^3_+ \to \mathbb{R}_+$ is given by

$$\begin{aligned}
L\aleph(S,\ I,\ R) =& \Lambda - \upsilon(S + I + R) - \delta_0 e^{-\upsilon\iota}\frac{I(t-\iota)}{S} - \frac{\Lambda}{S} + \frac{\gamma(I(t) - S(t))}{(1+\alpha_1 S(t))(1+\alpha_2 I(t))} - \lambda I(t) \\
&+ \frac{a}{1+bI(t)} - \frac{aI}{R(1+bI)} - \frac{\lambda I(t)}{R(t)} + \delta_0 e^{-\upsilon\iota}\frac{I(t-\iota)}{R} + 3\upsilon + \lambda + \delta + \frac{\eta_1^2 + \eta_2^2 + \eta_3^2}{2} \\
\leq& \Lambda + 3\upsilon + a + \lambda + \delta + \delta_0 + \frac{\gamma}{\alpha_2} + \frac{\eta_1^2 + \eta_2^2 + \eta_3^2}{2} := \tilde{M}.
\end{aligned}$$

Consequently,

$$d\aleph(S,\ I,\ R) \leq \tilde{M}dt + \eta_1(S - 1)dW_1(t) + \eta_2(I - 1)dW_2(t) + \eta_3(R - 1)dW_3(t).$$

Integration over $[0,\ \iota_\Gamma \wedge T = \min\{\iota_\Gamma,\ T\}]$ gives

$$\begin{aligned}
\int_0^{\iota_\Gamma\wedge T} d\aleph(S,\ I,\ R) \leq& \int_0^{\iota_\Gamma\wedge T}(S(r) - 1)A_1 dW_1(r) + \int_0^{\iota_\Gamma\wedge T}\tilde{M}dr + \int_0^{\iota_\Gamma\wedge T}\eta_2(I(r) - 1)dW_2(r) \\
&+ \int_0^{\iota_\Gamma\wedge T}\eta_3(R(r) - 1)dW_3(r).
\end{aligned}$$

Taking expectation, we obtain

$$\mathbb{E}\Big[\aleph(S(\iota_\Gamma \wedge T),\ I(\iota_\Gamma \wedge T),\ R(\iota_\Gamma \wedge T)\Big] \leq \aleph(S(0),\ I(0),\ R(0)) + \mathbb{E}\Big[\int_0^{\iota_\Gamma \wedge T} M dr\Big]$$
$$\mathbb{E}\Big[\aleph(S(\iota_\Gamma \wedge T),\ I(\iota_\Gamma \wedge T),\ R(\iota_\Gamma \wedge T)\Big] \leq \aleph(S(0),\ I(0),\ R(0)) + \tilde{M}T.$$

Let $\Xi_\Gamma = \{\iota_\Gamma \leq T\}\ \forall\ \Gamma \geq \Gamma_1$ and utilizing (5) then $\mathbb{P}(\Xi_\Gamma) \geq \varepsilon$. Fuhrer, noting that, $\forall\ \omega \in \Xi_\Gamma$ there is $S(\iota_\Gamma,\ \omega)$ or $I(\iota_\Gamma,\ \omega)$ or $R(\iota_\Gamma,\ \omega)$ that equal Γ or $\frac{1}{\Gamma}$, thus

$$\aleph(S(\iota_\Gamma,\ \omega),\ I(\iota_\Gamma,\ \omega),\ R(\iota_\Gamma,\ \omega)) \geq (\Gamma - 1 - \ln\Gamma) \wedge (\frac{1}{\Gamma} + \ln\Gamma - 1).$$

Therefore

$$\begin{aligned}
\aleph\Big(S(0),\ I(0),\ R(0)\Big) + \tilde{M}T &\geq \mathbb{E}\Big[1_{\Xi_\Gamma}(\omega)\aleph\Big(S(\iota_\Gamma \wedge T),\ I(\iota_\Gamma \wedge T),\ R(\iota_\Gamma \wedge T)\Big)\Big] \\
&= \mathbb{E}\Big[1_{\Xi_\Gamma}(\omega)\aleph\Big(S(\iota_\Gamma,\ \omega),\ I(\iota_\Gamma,\ \omega),\ R(\iota_\Gamma,\ \omega)\Big)\Big] \\
&\geq \mathbb{E}\Big[1_{\Xi_\Gamma}(\omega)(\Gamma - 1 - \ln\Gamma) \wedge \Big(\frac{1}{\Gamma} - 1 + \ln\Gamma\Big)\Big] \\
&\geq \mathbb{E}\Big[1_{\Xi_\Gamma}(\omega)\Big](\Gamma - 1 - \ln\Gamma) \wedge \Big(\frac{1}{\Gamma} - 1 + \ln\Gamma\Big) \\
&\geq \varepsilon(\Gamma - 1 - \ln\Gamma) \wedge \Big(\frac{1}{\Gamma} - 1 + \ln\Gamma\Big).
\end{aligned}$$

With $1_{\Xi_{\Gamma(\omega)}}$ representing as is indicator function of Ξ_Γ.

If $\Gamma \to \infty$, then $\infty = \aleph\Big(S(0),\ I(0),\ ,\ R(0)\Big) + \tilde{M}T < \infty$ yields a contradiction. It results that $\iota_\infty = \infty\ a.s$ □

2.2 Extinction criteria of infection

Our goal in this part is to find out sufficient conditions that are enough to make the disease disappear from the system (4).

Define a parameter

$$R_0 = \frac{\gamma}{\alpha_1(\upsilon + \lambda + \delta + \frac{\eta_2^2}{2})}.$$

Theorem 2 *(S(t), I(t), R(t)) be a solution of the model (4) with* $(S(0),\ I(0),\ R(0)) \in \mathbb{R}^3$,
if $R_0 < 1$ *then* $\limsup_{t\to\infty} \frac{\ln I(t)}{t} < 0$ *a.s., namely* $I(t) \longrightarrow 0$ *exponentially a.s.*

Proof Let us expressing the Martin–Crowley functional as follows

$$\begin{aligned}
\frac{\gamma S}{(1+\alpha_1 S)(1+\alpha_2 I)} =& \frac{\gamma\Lambda}{\upsilon + \alpha_1\Lambda} - \frac{\gamma\upsilon}{(\upsilon+\alpha_1\Lambda)(1+\alpha_1 S)(1+\alpha_2 I)}(\frac{\Lambda}{\upsilon} - S) - \frac{\gamma\Lambda\alpha_2 I}{(\upsilon+\alpha_1\Lambda)(1+\alpha_1 S)(1+\alpha_2 I)} \\
&- \frac{\gamma\Lambda\alpha_1\alpha_2 SI}{(\upsilon+\alpha_1\Lambda)(1+\alpha_1 S)(1+\alpha_2 I)} \\
=& \frac{\gamma\Lambda}{\upsilon + \alpha_1\Lambda} + \frac{\gamma\upsilon S}{(\upsilon+\alpha_1\Lambda)(1+\alpha_1 S)(1+\alpha_2 I)} - \frac{\gamma\Lambda}{(\upsilon+\alpha_1\Lambda)(1+\alpha_1 S)(1+\alpha_2 I)} \\
&- \frac{\gamma\Lambda\alpha_2 I}{(\upsilon+\alpha_1\Lambda)(1+\alpha_1 S)(1+\alpha_2 I)} - \frac{\gamma\Lambda\alpha_1\alpha_2 SI}{(\upsilon+\alpha_1\Lambda)(1+\alpha_1 S)(1+\alpha_2 I)} \\
\leq& \frac{\gamma\Lambda}{\upsilon + \alpha_1\Lambda} + \frac{\gamma\upsilon}{\alpha_1(\upsilon+\alpha_1\Lambda)} - \frac{\gamma\Lambda}{(\upsilon+\alpha_1\Lambda)(1+\alpha_1 S)(1+\alpha_2 I)} \\
&- \frac{\gamma\Lambda\alpha_2 I}{(\upsilon+\alpha_1\Lambda)(1+\alpha_1 S)(1+\alpha_2 I)} - \frac{\gamma\Lambda\alpha_1\alpha_2 SI}{(\upsilon+\alpha_1\Lambda)(1+\alpha_1 S)(1+\alpha_2 I)}.
\end{aligned} \tag{6}$$

Applying Itô formula, we get

$$d\ln I = \Big[\frac{\gamma S(t)}{(1+\alpha_1 S(t))(1+\alpha_2 I(t))} - \frac{a}{1+bI(t)} - (\delta + \upsilon + \lambda + \frac{\eta_2^2}{2})\Big]dt + \eta_2 dW_2(t).$$

By using (6), we obtain

$$d\ln I \leq \Big[\frac{\gamma\Lambda}{\upsilon + \alpha_1\Lambda} + \frac{\gamma\upsilon}{\alpha_1(\upsilon+\alpha_1\Lambda)} - (\upsilon + \delta + \lambda + \frac{\eta_2^2}{2})\Big]dt + \eta_2 dW_2(t)$$

$$= \left[\frac{\gamma}{\alpha_1} - (\upsilon + \delta + \lambda + \frac{\eta_2^2}{2})\right]dt + \eta_2 dW_2(t).$$

Integrating over $[0, t]$ and then diving by t yields

$$\frac{\ln I(t)}{t} \leq \frac{\gamma}{\alpha_1} - (\upsilon + \delta + \lambda + \frac{\eta_2^2}{2}) + \frac{\eta_2}{t}\int_0^t dW_3(r) + \frac{\ln I(0)}{t}.$$

Moreover, $\frac{1}{t}\int_0^t dW_2(r)$ is a continuous local martingale. By lemma (strong law) presented in [27], we obtain

$$\lim_{t\to\infty} \frac{1}{t}\int_0^t dW_2(r) = 0 \ \ a.s.$$

Taking $\lim_{t\to\infty}\sup$ of and if $R_0 < 1$ we get

$$\lim_{t\to\infty}\sup \frac{\ln I(t)}{t} \leq (\upsilon + \lambda + \delta + \frac{\eta_2^2}{2})(R_0 - 1) < 0.$$

This confirms that $\lim_{t\to\infty} I(t) = 0 \quad a.s.$ □

2.3 Ergodicity and stationary distribution of the system

Here, we carried out the analysis setting the certain criteria under which the system (4) has a SD. Let $\mathcal{Z}(t)$ represents a homogeneous Markov process in $\mathbb{R}^n$ explained by the SDE:

$$d\mathcal{Z}(t) = b(\mathcal{Z})dt + \sum_{r=1}^{k} \varrho_r(\mathcal{Z})dB_r(t)$$

The diffusion matrix is given by

$$\mathfrak{A}(x) = \left(\varsigma_{ij}(x)\right); \quad \varsigma_{ij}(x) = \sum_{r=1}^{k} \varrho_r^i(x)\varrho_r^j(x).$$

Lemma 1 [10] *The Markov process $\mathcal{Z}(t)$ admits a unique stationary distribution $\rho(.)$ if there exists a bounded region $\mathbb{V} \subset \mathbb{R}^n$ with a well-defined boundary Γ^* such that*

(a) There exists a positive constant $\mathcal{M}$ such that

$$\sum_{i,j=1}^{n} \varsigma_{ij}(x)\zeta_i\zeta_j \geq \mathcal{M}|\zeta|^2 \ x \in \mathbb{V}, \ \ \zeta \in \mathbb{R}^n.$$

(b) There exists a nonnegative C^2-function $\mathbb{U}$ and a neighborhood $\mathbb{V}$ such that, $L\mathbb{U}$ is negative for any $\mathbb{R}^n \setminus \mathbb{V}$.

Theorem 3 *If*

$$\bar{R}_0 := \frac{\gamma}{(\upsilon + \frac{\eta_1^2}{2})(\upsilon + \delta + \lambda + a + \frac{\eta_2^2}{2})} > 1,$$

then the solution of (4) has a unique SD $\rho(.)$, and further it possess the ergodicity.

Proof We will verify the conditions of lemma (1). Due the fact that the infectious class I in a local population randomly come into touch with the susceptible or the recovered, and because the infected retain have no recollection of their previous contacts, the solution of (4) shows a Markov process. Stated differently, there is no memory involved in the interactions between the infected and the susceptible or recovered. Furthermore, as the future state is not influenced by the past state, and only depends on the current state.

First, we show the condition (b). We will constructing a nonnegative C^2-function $\mathbb{U} : \mathbb{R}_+^3 \longrightarrow \mathbb{R}_+$.

Let

$$\mathbb{U}_1(S, I, R) = S + R + I - c_2 \ln I - c_1 \ln S,$$

where c_1, c_2, are positive constants, we will define later.

Using the Itô formula, we have

$$L(S + I + R) = \Lambda - \upsilon(S + I + R) - \lambda I$$

$$L(\ln S) = \frac{\Lambda}{S} - \frac{\gamma I(t)}{(1 + \alpha_1 S(t))(1 + \alpha_2 I(t))} - \upsilon + \delta_0 e^{-\upsilon\iota}\frac{I(t-\iota)}{S} - \frac{\eta_1^2}{2}$$

$$L(\ln I) = \frac{\gamma S(t)}{(1+\alpha_1 S(t))(1+\alpha_2 I(t))} - \frac{a}{1+bI(t)} - (\upsilon + \delta + \lambda + \frac{\eta_2^2}{2})$$
$$L(\ln R) = \frac{aI(t)}{(1+bI(t))R} - \upsilon - \frac{\eta_3^2}{2} + \delta\frac{I(t)}{R} - \delta_0 e^{-\upsilon\iota}\frac{I(t-\iota)}{R}.$$

Consequently,

$$\begin{aligned} L\mathbb{U}_1 &= \Lambda - \upsilon(S+I+R) - \lambda I - \frac{c_1\Lambda}{S} + \frac{c_1\gamma I(t)}{(1+\alpha_1 S(t))(1+\alpha_2 I(t))} - c_1\delta_0 e^{-\upsilon\iota}\frac{I(t-\iota)}{S} + c_1\left(\upsilon + \frac{\eta_1^2}{2}\right) \\ &\quad - \frac{c_2\gamma S(t)}{(1+\alpha_1 S(t))(1+\alpha_2 I(t))} + \frac{c_2 a}{1+bI(t)} + c_2\left(\upsilon + \delta + \lambda + \frac{\eta_2^2}{2}\right) \\ &\quad + (1+\alpha_1 S(t))(1+\alpha_2 I(t)) - (1+\alpha_1 S(t))(1+\alpha_2 I(t)). \\ L\mathbb{U}_1 &\le -3\sqrt[3]{\gamma\Lambda c_1 c_2} + \Lambda + c_1(\upsilon + \frac{\eta_1^2}{2}) + c_2(\upsilon + \delta + \lambda + a + \frac{\eta_2^2}{2}) + (1+\alpha_1 S(t))(1+\alpha_2 I(t)) \\ &\quad + \frac{c_1\gamma I(t)}{(1+\alpha_1 S(t))(1+\alpha_2 I(t))}. \end{aligned}$$

Letting

$$\Lambda = c_1\left(\upsilon + \frac{\eta_1^2}{2}\right) = c_2\left(\upsilon + \delta + \lambda + a + \frac{\eta_2^2}{2}\right),$$

then

$$c_1 = \frac{\Lambda}{(\upsilon + \frac{\eta_1^2}{2})}, \quad c_2 = \frac{\Lambda}{(\upsilon + \delta + \lambda + a + \frac{\eta_2^2}{2})}.$$

As a result

$$\begin{aligned} L\mathbb{U}_1 &\le -3\sqrt[3]{\frac{\gamma\Lambda^3}{(\upsilon + \frac{\eta_1^2}{2})(\upsilon + \delta + \lambda + a + \frac{\eta_2^2}{2})}} + 3\Lambda + (1+\alpha_1 S(t))(1+\alpha_2 I(t)) + \frac{c_1\gamma I(t)}{(1+\alpha_1 S(t))(1+\alpha_2 I(t))} \\ &\le -3\Lambda\left(\sqrt[3]{\frac{\gamma}{(\upsilon + \frac{\eta_1^2}{2})(\upsilon + \delta + \lambda + a + \frac{\eta_2^2}{2})}} - 1\right) + \frac{\gamma\Lambda}{\alpha_2(\upsilon + \frac{\eta_1^2}{2})} + (1+\alpha_1 S(t))(1+\alpha_2 I(t)) \\ &= -3\Lambda\left[(R_0^s)^{\frac{1}{3}} - 1\right] + \frac{\gamma\Lambda}{\alpha_2(\upsilon + \frac{\eta_1^2}{2})} + (1+\alpha_1 S(t))(1+\alpha_2 I(t)). \end{aligned}$$

We define

$$\mathbb{U}_2(S,\, I,\, R) = c_3(S + R + I - c_2\ln I - c_1\ln S) + S + R + I - \ln S - \ln I - \ln R,$$

where c_3 is constant satisfying the following condition

$$-3\Lambda c_3\left[(R_0^s)^{\frac{1}{3}} - 1\right] + \Lambda + \frac{\gamma}{\alpha_2} + a + 3\upsilon + \delta + \lambda + \frac{\eta_2^2 + \eta_3^2}{2} < -2.$$

Obviously

$$\liminf_{q\to+\infty,\,(S,I,R)\in\mathbb{R}_+^3\setminus\mathbb{V}_q} \mathbb{U}_2(S,\, I,\, R) = +\infty$$

where $\mathbb{V}_q =]\frac{1}{q}, q[\times]\frac{1}{q}, q[\times]\frac{1}{q}, q[$.

Since: when $q \to +\infty$, $(S,\, I,\, R) \in \mathbb{R}_+^3\setminus\mathbb{V}_q$ is exactly equal to
$\{0\} \times [0, +\infty[\times[0, +\infty[\cup[0, +\infty[\times\{0\} \times [0, +\infty[\cup[0, +\infty[\times[0, +\infty[\times\{0\}$.

Besides, we have

$$\frac{\partial\mathbb{U}_2(S,\, I,\, R)}{\partial S} = c_3 + 1 - \frac{c_3c_1 + 1}{S}, \qquad \frac{\partial\mathbb{U}_2(S,\, I,\, R)}{\partial I} = c_3 + 1 - \frac{c_3c_2 + 1}{I}, \qquad \frac{\partial\mathbb{U}_2(S,\, I,\, R)}{\partial R} = c_3 + 1 - \frac{1}{R},$$

the function $\mathbb{U}_2$ has unique stagnation point $(S_*,\, I_*,\, R_*) = \left(\frac{c_3c_1 + 1}{c_3 + 1},\, \frac{c_3c_2 + 1}{c_3 + 1},\, \frac{1}{c_3 + 1}\right)$ The Hessian matrix of $\mathbb{U}_2$ at $(S_*,\, I_*,\, R_*)$ is given by

$$\mathbb{H} = \begin{bmatrix} \frac{c_3c_1+1}{S_*^2} & 0 & 0 \\ 0 & \frac{c_3c_2+1}{I_*^2} & 0 \\ 0 & 0 & \frac{1}{R_*^2} \end{bmatrix}.$$

$\mathbb{H}$ is positive definite and $\mathbb{U}_2$ is continues function; then, it is clear that $\mathbb{U}_2$ has a unique minimum $(S_*,\ I_*,\ R_*) \in \mathbb{R}^3_+$.

Let

$$\mathbb{U}(S,\ I,\ R) = \mathbb{U}_2(S,\ I,\ R) - \mathbb{U}_2(S_*,\ I_*,\ R_*).$$

Utilizing Itô criteria to obtain

$$\begin{aligned} L\mathbb{U}(S,\ I,\ R) =& L\mathbb{U}_2(S,\ I,\ R) \\ \leq& -3\Lambda c_3\Big[(R_0^s)^{\frac{1}{3}} - 1\Big] + \frac{c_3\gamma\Lambda}{\alpha_2(\upsilon + \frac{\eta_1^2}{2})} + c_3(1+\alpha_1 S(t))(1+\alpha_2 I(t)) - \upsilon(S+I+R) + \Lambda - \lambda I \\ & - \frac{\Lambda}{S} + \frac{\gamma I(t)}{(1+\alpha_1 S(t))(1+\alpha_2 I(t))} + \upsilon + \frac{\eta_1^2}{2} - \frac{\gamma S(t)}{(1+\alpha_1 S(t))(1+\alpha_2 I(t))} - \delta_0 e^{-\upsilon\iota}\frac{I(t-\iota)}{S} \\ & + \frac{a}{1+bI(t)} + (\delta + \upsilon + \lambda + \frac{\eta_2^2}{2}) - \frac{aI(t)}{(1+I(t)b)R} + \upsilon + \frac{\eta_3^2}{2} - \delta\frac{I(t)}{R} + \delta_0 e^{-\upsilon\iota}\frac{I(t-\iota)}{R}. \end{aligned}$$

Let $\varepsilon_l > 0$, $l = 1, 2, ..., 5$, we give a closed and bounded set

$$\mathbb{V} = \Big\{(S,\ I,\ R) \in \mathbb{R}^3_+ : \varepsilon_1 \leq S \leq \frac{1}{\varepsilon_2},\ \varepsilon_3 \leq I \leq \frac{1}{\varepsilon_4},\ \varepsilon_3^2 \leq R \leq \frac{1}{\varepsilon_5}\Big\}.$$

We can choose $\varepsilon_l, l = 1, 2, ..., 5$ such that the subsequent criteria hold

- $-\frac{\Lambda}{\varepsilon_1} + \urcorner_1 < -1$
- $-3\Lambda c_3\Big[(R_0^s)^{\frac{1}{3}} - 1\Big] + c_3(1+\alpha_1 S)(1+\alpha_2\varepsilon_3) + \urcorner_2 < -1$
- $-\frac{\delta}{\varepsilon_3} + \urcorner_1 < -1$,
- $-\frac{\upsilon}{\varepsilon_2} + \urcorner_1 < -1$,
- $-\frac{\upsilon}{\varepsilon_4} + \urcorner_1 < -1$,
- $-\frac{\upsilon}{\varepsilon_5} + \urcorner_1 < -1$,

where

$$\urcorner_1 = \sup\Big\{\frac{c_3\gamma\Lambda}{\alpha_2(\upsilon + \frac{\eta_1^2}{2})} + c_3(1+\alpha_1 S)(1+\alpha_2 I) + \Lambda + \frac{\gamma}{\alpha_2} + a + 3\upsilon + \delta + \lambda + \frac{\eta_2^2}{2} + \frac{\eta_3^2}{2}\Big\},$$

and

$$\urcorner_2 = \frac{c_3\gamma\Lambda}{\alpha_2(\upsilon + \frac{\eta_1^2}{2})} + \Lambda + \frac{\gamma}{\alpha_2} + a + 3\upsilon + \delta + \lambda + \frac{\eta_2^2 + \eta_3^2}{2}.$$

Next, we show that $L\mathbb{U} < 0$ on $\mathbb{R}^3_+\backslash\mathbb{V}$, $\mathbb{R}^3_+\backslash\mathbb{V} = \bigcup_{j=1}^6 \mathbb{V}_j$, where

$$\begin{aligned} \mathbb{V}_1 &= \Big\{(S,\ I,\ R) \in \mathbb{R}^3_+,\ 0 < S < \varepsilon_1\Big\}, \quad \mathbb{V}_2 = \Big\{(S,\ I,\ R) \in \mathbb{R}^3_+,\ 0 < I < \varepsilon_3,\ S > 0\Big\}, \\ \mathbb{V}_3 &= \Big\{(S,\ I,\ R) \in \mathbb{R}^3_+,\ 0 < R < \varepsilon_3^2,\ I > \varepsilon_3\Big\}, \quad \mathbb{V}_4 = \Big\{(S,\ I,\ R) \in \mathbb{R}^3_+,\ S > \frac{1}{\varepsilon_2}\Big\}, \\ \mathbb{V}_5 &= \Big\{(S,\ I,\ R) \in \mathbb{R}^3_+,\ I > \frac{1}{\varepsilon_4}\Big\}, \quad \mathbb{V}_6 = \Big\{(S,\ I,\ R) \in \mathbb{R}^3_+,\ R > \frac{1}{\varepsilon_5}\Big\}. \end{aligned}$$

Case i. For $(S,\ I,\ R) \in \mathbb{V}_1$

$$L\mathbb{U}(S,\ I,\ R) \leq \urcorner_1 - \frac{\Lambda}{S} \leq \urcorner_1 - \frac{\Lambda}{\varepsilon_1} < -1.$$

Case ii. For $(S,\ I,\ R) \in \mathbb{V}_2$

$$\begin{aligned} L\mathbb{U}(S,\ I,\ R) \leq& -3\Lambda c_3\Big[(R_0^s)^{\frac{1}{3}} - 1\Big] + c_3(1+\alpha_1 S)(1+\alpha_2 I) + \urcorner_2 \\ \leq& -3\Lambda c_3\Big[(R_0^s)^{\frac{1}{3}} - 1\Big] + c_3(1+\alpha_1 S)(1+\alpha_2\varepsilon_3) + \urcorner_2 < -1. \end{aligned}$$

Case iii. For $(S,\ I,\ R) \in \mathbb{V}_3$

$$L\mathbb{U}(S,\ I,\ R) \leq \urcorner_1 - \delta\frac{I}{R} \leq \urcorner_1 - \frac{\delta}{\varepsilon_3} < -1.$$

Case iv. For $(S,\ I,\ R) \in \mathbb{V}_4$

$$L\mathbb{U}(S,\ I,\ R) \leq \urcorner_1 - \upsilon S \leq \urcorner_1 - \frac{\upsilon}{\varepsilon_2} < -1.$$

Case v. For $(S,\ I,\ R) \in \mathbb{V}_5$

$$L\mathbb{U}(S,\ I,\ R) \leq \urcorner_1 - \upsilon I \leq \urcorner_1 - \frac{\upsilon}{\varepsilon_4} < -1.$$

Case vi. For $(S,\ I,\ R) \in \mathbb{V}_6$

$$L\mathbb{U}(S,\ I,\ R) \leq \urcorner_1 - \upsilon R \leq \urcorner_1 - \frac{\upsilon}{\varepsilon_5} < -1.$$

Next, we prove the criteria stated in (a). The diffusion matrix corresponds to (4) is as follows

$$\begin{bmatrix} \eta_1^2 S^2 & 0 & 0 \\ 0 & \eta_2^2 I^2 & 0 \\ 0 & 0 & \eta_3^2 R^2 \end{bmatrix},$$

and

$$\sum_{i,\,j=1}^{3} \varsigma_{ij}(S,\ I,\ R)\zeta_i\zeta_j = \eta_1^2 S^2\zeta_1^2 + \eta_2^2 I^2\zeta_2^2 + \eta_3^2 R^2\zeta_3^2$$
$$\geq \mathcal{M}|\zeta|^2 \ \text{ for all } \ (S,\ I,\ R) \in \mathbb{V},\ \zeta \in \mathbb{R}_+^3,$$

where $\mathcal{M} = \min\{\eta_1^2 S^2,\ \eta_2^2 I^2,\ \eta_3^2 R^2\}$.

From what has been shown above, we conclude that model (4) has a unique ergodic SD $\rho(.)$. □

3 Probability density function (PDF) analysis

Since the statistical features of system (4) cannot be reflected by the existence of a stationary solution, the purpose of this section is to determine the corresponding PDF with regard to the stationary solution to system (4). Prior to doing so, we must provide two equivalent system (4) transformations.

Consider the n-dimensional stochastic differential equation defined as follows:

$$dX(t) = f(X(t))dt + g(X(t))dW(t), \quad t \geq 0.$$

where $f(X(t))$ is function in $\mathbb{R}^n$ and $g(X(t))$ is a $n \times m$ matrix.

If there is a point $X^* \in \mathbb{R}_+^n/\{0\}$ such that the following equation is satisfied:

$$f(X^*) = 0,$$

we say that X^* is a quasi-endemic equilibrium point.

Let $(\upsilon_1,\ \upsilon_2,\ \upsilon_3) = (\ln S,\ \ln I,\ \ln R)$, by Ito's formula, model (4) can be written as

$$\begin{aligned}
d\upsilon_1(t) &= \Big[\Lambda e^{-\upsilon_1} - \frac{\gamma e^{\upsilon_2}}{(1+\alpha_1 e^{\upsilon_1})(1+\alpha_2 e^{\upsilon_2})} - \upsilon + \delta_0 e^{\upsilon_2(t-\iota)-\upsilon_1-\upsilon\iota} - \frac{\eta_1^2}{2}\Big]dt + \eta_1 dW_1(t),\\
d\upsilon_2(t) &= \Big[\frac{\gamma e^{\upsilon_1}}{(1+\alpha_1 e^{\upsilon_1})(1+\alpha_2 e^{\upsilon_2})} - \frac{a}{1+be^{\upsilon_2}} - (\upsilon+\delta+\lambda) - \frac{\eta_2^2}{2}\Big]dt + \eta_2 dW_2(t),\\
d\upsilon_3(t) &= \Big[\frac{ae^{\upsilon_2-\upsilon_3}}{1+be^{\upsilon_2}} - \upsilon + \delta e^{\upsilon_2-\upsilon_3} - \delta_0 e^{\upsilon_2(t-\iota)-\upsilon_3-\upsilon\iota} - \frac{\eta_3^2}{2}\Big]dt + \eta_3 dW_3(t),
\end{aligned} \tag{7}$$

then, we can find a unique and quasi-endemic equilibrium point $\mathcal{E}^* = (S^*, I^*, R^*) := (e^{v_1^*}, e^{v_2^*}, e^{v_3^*})$, which is determined by the following: evaluate at $\iota = 0$

$$\begin{aligned} 0 &= \Lambda e^{-v_1^*} - \frac{\gamma e^{v_2^*}}{(1+\alpha_1 e^{v_1^*})(1+\alpha_2 e^{v_2^*})} - \upsilon + \delta_0 e^{v_2^*(t)-v_1^*} - \frac{\eta_1^2}{2}, \\ 0 &= \frac{\gamma e^{v_1^*}}{(1+\alpha_1 e^{v_1^*})(1+\alpha_2 e^{v_2^*})} - \frac{a}{1+be^{v_2^*}} - (\delta+\upsilon+\lambda) - \frac{\eta_2^2}{2}, \\ 0 &= \frac{ae^{v_2^*-v_3^*}}{1+be^{v_2^*}} - \upsilon + \delta e^{v_2^*-v_3^*} - \delta_0 e^{v_2^*(t)-v_3^*} - \frac{\eta_3^2}{2}. \end{aligned} \tag{8}$$

We obtain

$$S^* = \frac{(\delta+\upsilon+\lambda+\frac{\eta_2^2}{2})\alpha_2 bI^{*^2} + [(\delta+\upsilon+\lambda+\frac{\eta_2^2}{2})(\alpha_2+b) + a\alpha_2]I^* + (\upsilon+\delta+\lambda+\frac{\eta_2^2}{2}) + a}{(\upsilon+\delta+\lambda+\frac{\eta_2^2}{2})\alpha_1\alpha_2 bI^{*^2} + [\gamma b - (\delta+\upsilon+\lambda+\frac{\eta_2^2}{2})\alpha_1(\alpha_2+b) - a\alpha_1\alpha_2]I^* + \gamma - (\delta+\upsilon+\lambda+\frac{\eta_2^2}{2})\alpha_1 - a\alpha_1},$$

$$R^* = \frac{(\delta-\delta_0)bI^{*^2} + (\delta-\delta_0+a)I^*}{(\upsilon+\frac{\eta_3^2}{2})bI^* + (\upsilon+\frac{\eta_3^2}{2})},$$

and I^* satisfies eq. (9)

$$\Theta_1 I^{*^5} + \Theta_2 I^{*^4} + \Theta_3 I^{*^3} + \Theta_4 I^{*^2} + \Theta_5 I^* + \Theta_6 = 0, \tag{9}$$

with

$$\begin{aligned} \Theta_1 &= \gamma A_2^2\alpha_1\alpha_2^2 b^2 + \psi_1\delta_0\alpha_1\alpha_2 + \psi_2\delta_0\alpha_2, \\ \Theta_2 &= -2A_1A_2\alpha_2^2 b\alpha_1(A_2\alpha_2 + A_2 b + a\alpha_2) + \psi_1(\delta_0\alpha_1 + \Lambda + \alpha_1\alpha_2 - \gamma - A_1\alpha_2) + \psi_2(\delta_0 + \Lambda\alpha_2) \\ &\quad + \delta_0\alpha_1\alpha_2(F_1\xi_3 + F_2\xi_2 + F_3\xi_1) + \delta_0\alpha_2(2\xi_1\xi_3 + \xi_2^2), \\ \Theta_3 &= -2A_1A_2\alpha_2 b\alpha_1(A_2\alpha_2 + A_2 b + a\alpha_2) + \psi_1(\Lambda\alpha_1 - A_1) + \psi_2\Lambda - A_1(2F_1F_3 + F_2^2)\alpha_1\alpha_2 \\ &\quad + (F_1\xi_3 + F_2\xi_2 + F_3\xi_1)(\delta_0\alpha_1 + \Lambda\alpha_1\alpha_2 - \gamma - A_1\alpha_2) + (\delta_0\alpha_1\alpha_2(F_2\xi_3 + F_3\xi_2)) + 2\xi_2\xi_3\delta_0\alpha_2 \\ &\quad + (\delta_0 + \Lambda\alpha_2)(2\xi_1\xi_3 + \xi_2^2), \\ \Theta_4 &= -A_1(2F_1F_3 + F_2^2)\alpha_1 + \Lambda(2\xi_1\xi_3 + \xi_2^2) + (F_1\xi_3 + F_2\xi_2 + F_3\xi_1)(\Lambda\alpha_1 - A_1) - 2A_1F_2F_3\alpha_1\alpha_2 \\ &\quad + 2\xi_2\xi_3(\delta_0 + \Lambda\alpha_2) + (F_2\xi_2 + F_3\xi_2)(\delta_0\alpha_1 + \Lambda\alpha_1\alpha_2 - \gamma - A_1\alpha_2) + F_3\xi_3\delta_0\alpha_1\alpha_2 + \xi_3^2\delta_0\alpha_2, \\ \Theta_5 &= -A_1F_3^2\alpha_1\alpha_2 + \xi_3^2(\delta_0 + \Lambda\alpha_2) + F_3\xi_3(\delta_0\alpha_1 + \Lambda\alpha_1\alpha_2 - \gamma - A_{1\alpha_2}) - 2A_1F_2F_3\alpha_1 + (F_2\xi_3 \\ &\quad + F_3\xi_2)(\Lambda\alpha_1 - A_1) + 2\xi_2\xi_3\Lambda, \\ \Theta_6 &= -A_1F_3^2\alpha_1 + F_3\xi_3(\Lambda\alpha_1 - A_1) + \Lambda\xi_3^2, \end{aligned}$$

and

$$\begin{aligned} &A_1 = \upsilon + \frac{\eta_1^2}{2},\ A_2 = \upsilon + \delta + \lambda + \frac{\eta_2^2}{2},\ A_3 = \upsilon + \frac{\eta_3^2}{2}, \\ &\psi_1 = A_2\alpha_2 b(\gamma b - A_2\alpha_1\alpha_2 - A_2\alpha_1 b - a\alpha_1\alpha_2) - A_2\alpha_1\alpha_2 b(A_2\alpha_2 + A_2 b + a\alpha_2), \\ &\psi_2 = -2A_2\alpha_1\alpha_2 b(\gamma b - A_2\alpha_1\alpha_2 - A_2\alpha_1 b - a\alpha_1\alpha_2), \\ &F_1 = A_2\alpha_2 b,\quad F_2 = A_2\alpha_2 + A_2 b + a\alpha_2,\quad F_3 = A_2 + a, \\ &\xi_1 = -A_2\alpha_1\alpha_2 b,\quad \xi_2 = \gamma b - A_2\alpha_1\alpha_2 - A_2\alpha_1 b - a\alpha_1\alpha_2,\quad \xi_3 = \gamma - A_2\alpha_1 - a\alpha_1. \end{aligned}$$

According to Descarte's rule of signs [28], we obtain the following:

- $\Theta_i > 0,\ for\ i = 1, ..5,\ and\ \Theta_6 < 0.$
- $\Theta_i > 0,\ for\ i = 1, ..4,\ and\ \Theta_5 < 0,\ \Theta_6 < 0.$
- $\Theta_i > 0,\ for\ i = 1, ..3,\ and\ \Theta_4 < 0,\ \Theta_5 < 0,\ \Theta_6 < 0.$
- $\Theta_1 > 0,\ \Theta_2 > 0,\ \Theta_3 < 0,\ \Theta_4 < 0,\ \Theta_5 < 0,\ \Theta_6 < 0.$
- $\Theta_1 > 0,\ \Theta_i < 0,\ for\ i = 2, ..6.$

If either condition mentioned above is fulfilled, then eq. (9) has a unique root $I^* > 0$. Thus, there exists a unique $\mathcal{E}^*$.

Next, let $y_i = v_i - v_i^*$, for $i = 1, 2, 3,$, then system obtained by the linearization of the model (7) around $\mathcal{E}^*$ as follows

$$\begin{aligned} dy_1(t) &= (-a_1 y_1 - (a_2 + a_3)y_2)dt + \eta_1 dW_1(t), \\ dy_2(t) &= (a_4 y_1 - a_5 y_2)dt + \eta_2 dW_2(t), \\ dy_3(t) &= ((a_6 + a_7)y_2 - a_8 y_3)dt + \eta_3 dW_3(t), \end{aligned} \tag{10}$$

where

$$a_1 = \frac{-\alpha_1\gamma S^* I^*}{(1+\alpha_1 S^*)^2(1+\alpha_2 I^*)} + \frac{(\Lambda+\delta_0 I^*)}{S^*},\quad a_2 = \frac{\gamma I^*}{(1+\alpha_1 S^*)(1+\alpha_2 I^*)},\quad a_3 = \frac{-\delta_0 I^*}{S^*},$$
$$a_4 = \frac{\gamma S^*}{(1+\alpha_1 S^*)^2(1+\alpha_2 I^*)},\ a_5 = \frac{-abI^*}{(1+bI^*)^2} + \frac{\alpha_2\gamma S^* I^*}{(1+\alpha_1 S^*)(1+\alpha_2 I^*)^2},\quad a_6 = \frac{aI^*}{R^*(1+bI^*)^2} + \frac{\delta I^*}{R^*},$$
$$a_7 = \frac{-\delta_0}{R^*},\quad a_8 = \frac{aI^*}{R^*(1+bI^*)} + \frac{\delta I^* - \delta_0}{R^*}.$$

3.1 PDF of SD analysis

Lemma 2 [29] *Consider the three-dimensional equation as follows*

$$A_0^2 + M_0 Q_0 + Q_0 M_0^T = 0,$$

where

$$A_0 = \begin{pmatrix} 1 & 0 & 0 \\ 0 & 0 & 0 \\ 0 & 0 & 0 \end{pmatrix},\quad M_0 = \begin{pmatrix} -b_1 & -b_2 & -b_3 \\ 1 & 0 & 0 \\ 0 & 1 & 0 \end{pmatrix}.$$

If M_0 is a Hurwitz matrix, that is $b_1 > 0$, $b_3 > 0$, and $b_1 b_2 - b_3 > 0$, then Q_0 is positive definite, and

$$Q_0 = \frac{1}{2(b_1 b_2 - b_3)} \begin{pmatrix} b_2 & 0 & -1 \\ 1 & 1 & 0 \\ -1 & 0 & \frac{b_1}{b_3} \end{pmatrix}.$$

Clearly, b_1, b_2 and b_3 are the coefficient of the characteristic polynomial $P_{M_0}(\varkappa) = \varkappa^3 + b_1\varkappa^2 + b_2\varkappa + b_3$

Lemma 3 [29] *Consider the equation given below*

$$A_0^2 + H_0\Phi_0 + \Phi_0 H_0^T = 0$$

where

$$A_0 = \begin{pmatrix} 1 & 0 & 0 \\ 0 & 0 & 0 \\ 0 & 0 & 0 \end{pmatrix},\quad H_0 = \begin{pmatrix} -\varpi_1 & -\varpi_2 & -\varpi_3 \\ 1 & 0 & 0 \\ 0 & 0 & h_{33} \end{pmatrix}.$$

If $\varpi_1 > 0$ and $\varpi_2 > 0$, then Φ_0 is semi-positive definite, and

$$\Phi_0 = \begin{pmatrix} \frac{1}{2\varpi_1} & 0 & 0 \\ 0 & \frac{1}{2\varpi_1\varpi_2} & 0 \\ 0 & 0 & 0 \end{pmatrix}.$$

Remark 1 From [29], M_0 and H_0 are called standard $\mathcal{R}_1$ and $\mathcal{R}_2$ matrices, respectively.

Lemma 4 [30] *For the following three-dimensional equation*

$$D_0^2 + D_1 L_0 + L_0 D_1^T = 0,$$

where L_0 is symmetric matrix $D_0 = diag(d_0, 0, 0)$ and $(d_0 \neq 0)$,

$$D_1 = \begin{pmatrix} d_1 & d_2 & d_3 \\ 0 & d_4 & d_5 \\ 0 & d_6 & d_7 \end{pmatrix}.$$

If $d_1 < 0$, then L_0 is a positive semi-definite matrix in the form $L_0 = diag(\frac{-d_0^2}{2d_1}, 0, 0)$.

Theorem 4 *Let be (S(0), I(0), R(0)) $\in \mathbb{R}_+^3$ an initial value, if*

$$\min\left\{\frac{\upsilon\alpha_1\alpha_2}{\gamma}, \frac{\gamma}{(1+\alpha_1\frac{\Lambda}{\upsilon})(1+\alpha_2\frac{\Lambda}{\upsilon})\delta_0\frac{\Lambda}{\upsilon}}, \frac{\alpha_2\gamma}{a(1+\alpha_1\frac{\Lambda}{\upsilon})(1+\alpha_2\frac{\Lambda}{\upsilon})^2}, \frac{\delta}{\delta_0}\right\} > 1. \tag{11}$$

then model (4) posses a PDF

$$\varphi(S, I, R) = (2\pi)^{-\frac{3}{2}}|Q|^{-\frac{1}{2}}\exp(-\frac{1}{2}(\ln\frac{S}{S^*}, \ln\frac{I}{I^*}, \ln\frac{R}{R^*})Q^{-1}(\ln\frac{S}{S^*}, \ln\frac{I}{I^*}, \ln\frac{R}{R^*})^T).$$

The special structure of matrix Q which is positive definite is given below.

Proof For simplicity, let $W(t) = (W_1(t),\ W_2(t),\ W_3(t))^T$, $A = diag(\eta_1,\ \eta_2,\ \eta_3)$, and

$$M = \begin{pmatrix} -a_1 & -(a_2+a_3) & 0 \\ a_4 & -a_5 & 0 \\ 0 & a_7+a_6 & -a_8 \end{pmatrix}.$$

Therefore, system (10) can be rewritten as $dY = MY + AdW(t)$. By Gardiner [31] (in page 96), a unique DF $\varphi(Y)$ at the quasi EE fulfills the following Fokker–Planck equation:

$$-\sum_{j=1}^{3}\frac{\eta_j}{2}\frac{\partial^2\varphi}{\partial y_j^2} + \frac{\partial}{\partial y_1}([-a_1y_1 - (a_2+a_3)y_2]\varphi) + \frac{\partial}{\partial y_2}([a_4y_1 - a_5y_2]\varphi) + \frac{\partial}{\partial y_1}([(a_6+a_7)y_2 - a_8y_3]\varphi) = 0,$$

based on Roozen [32], that can be approximated via the Gaussian distribution

$$\varphi(Y) = ce^{-\frac{1}{2}YHY^T},$$

where $c > 0$ which is determined from

$$\int_{\mathbb{R}^3}\varphi(Y)dY = 1,$$

and H is a symmetric matrix satisfying

$$HA^2H + HM + M^TH = 0.$$

If H represents the inversion matrix, let $Q = H^{-1}$, then we get

$$A^2 + MQ + QM^T = 0. \tag{12}$$

Moreover, the corresponding constant value is calculated as $c = (2\pi)^{-\frac{3}{2}}$.

Next, to show that matrix Q is positive definite it sufficient to prove that M has eigenvalues with negative real parts. Further, the characteristic polynomial is constructed as below

$$P_M(r) = r^3 + p_1r^2 + p_2r + p_3,$$

where

$$p_1 = a_1 + a_5 + a_8, \quad p_2 = a_1a_5 + a_4(a_2+a_3) + a_8(a_1+a_5), \quad p_3 = a_8a_1a_5 + a_8a_4(a_2+a_3).$$

By (11) it can be shown that

$$-a_1 = \frac{\alpha_1\gamma S^*I^*}{(1+\alpha_1S^*)^2(1+\alpha_2I^*)} - \frac{(\Lambda+\delta_0I^*)}{S^*} \le \frac{\gamma}{\alpha_1\alpha_2} - \upsilon < 0, \tag{13}$$

$$-(a_2+a_3) = \frac{\delta_0I^*}{S^*} - \frac{\gamma I^*}{(1+\alpha_1S^*)(1+\alpha_2I^*)} \le \delta_0\frac{\Lambda}{\upsilon} - \frac{\gamma}{(1+\alpha_1\frac{\Lambda}{\upsilon})(1+\alpha_2\frac{\Lambda}{\upsilon})} < 0, \tag{14}$$

$$-a_5 = \frac{abI^*}{(1+bI^*)^2} - \frac{\alpha_2\gamma S^*I^*}{(1+\alpha_1S^*)(1+\alpha_2I^*)^2}) \le a - \frac{\alpha_2\gamma}{(1+\alpha_1\frac{\Lambda}{\upsilon})(1+\alpha_2\frac{\Lambda}{\upsilon})^2} < 0, \tag{15}$$

$$a_6 + a_7 = \frac{aI^*}{R^*(1+bI^*)^2} + \frac{\delta I^*}{R^*} - \frac{\delta_0}{R^*} \ge \frac{\delta\upsilon}{\Lambda} - \delta_0\frac{\Lambda}{\upsilon} > 0, \tag{16}$$

$$-a_8 = \frac{-aI^*}{R^*(1+bI^*)} - \frac{\delta I^* - \delta_0}{R^*} \le \delta_0\frac{\Lambda}{\upsilon} - \frac{\delta\upsilon}{\Lambda} < 0. \tag{17}$$

Consequently, from (13) to (17), we obtain

$$\begin{aligned} &p_i > 0, \quad i = 1,2,3 \quad \text{and} \\ &p_1p_2 - p_3 = a_8^2(a_1+a_5) + (a_1+a_5)(a_1a_5 + a_4(a_2+a_3) + a_8(a_1+a_5)) > 0. \end{aligned} \tag{18}$$

So, by (18) and using Lemma (2.6) in [30], then Q of eq.(12) is positive definite.

Based on the finite independent superposition principle [33], eq. (12) can be written as follows:

$$A_j^2 + MQ_j + Q_jM^T = 0, \ \ (j = 1,2,3,) \tag{19}$$

where

$$A_1 = diag(\eta_1, 0, 0),\ A_2 = diag(0, \eta_2, 0),\ A_3 = diag(0, 0, \eta_3),\ Q = Q_1 + Q_2 + Q_3,\ \text{and}\ A^2 = A_1^2 + A_2^2 + A_3^2.$$

Next, the special formula of Q is obtained by the following steps

Step 1. For eq. (20)

$$A_1^2 + MQ_1 + Q_1M^T = 0. \tag{20}$$

Let

$$M_1 = B_1 M B_1^{-1}.$$

Letting $M_1 = B_1 M B_1^{-1}$, where

$$B_1 = \begin{bmatrix} a_4(a_6+a_7) & -(a_5+a_8)(a_6+a_7) & a_8^2 \\ 0 & a_6+a_7 & -a_8 \\ 0 & 0 & 1 \end{bmatrix},$$

is the standard transform matrix, can be derived using the method (I) presented in [29], according to the uniqueness of the standard $\mathcal{R}_1$ matrix of M, we have that

$$M_1 = \begin{bmatrix} -p_1 & -p_2 & -p_3 \\ 1 & 0 & 0 \\ 0 & 1 & 0 \end{bmatrix},$$

where p_1, p_2 and p_3 are the same as we mentioned above.

Next, eq. (20) can be written as follows

$$B_1 A_1^2 B_1^T + M_1 B_1 Q_1 B_1^T + B_1 Q_1 B_1^T M_1^T = 0. \tag{21}$$

Letting

$$\Phi_1 = \frac{1}{q_1^2} B_1 Q_1 B_1^T,\quad q_1 = a_4(a_6+a_7)\eta_1,$$

eq. (21) becomes

$$A_0^2 + M_1\Phi_1 + \Phi_1 M_1^T = 0.$$

By Lemma (2), Φ_1 is positive definite, it is given in the following form

$$\Phi_1 = \frac{1}{2(p_1p_2 - p_3)} \begin{pmatrix} p_2 & 0 & -1 \\ 1 & 1 & 0 \\ -1 & 0 & \frac{p_1}{p_3} \end{pmatrix}.$$

Therefore,

$$Q_1 = q_1^2 B_1^{-1} \Phi_1 (B_1^T)^{-1},$$

is positive definite

Step 2. Consider the following equation

$$A_2^2 + MQ_2 + Q_2M^T = 0. \tag{22}$$

Similarly, taking

$$C_2 = (B_3B_2)M(B_3B_2)^{-1},$$

where the matrix B_2 and B_3 are given by

$$B_2 = \begin{bmatrix} 0 & 1 & 0 \\ 0 & 0 & 1 \\ 1 & 0 & 0 \end{bmatrix},\ B_3 = \begin{bmatrix} 1 & 0 & 0 \\ 0 & 1 & 0 \\ 0 & \frac{(a_2+a_3)}{(a_6+a_7)} & 1 \end{bmatrix}.$$

By simple computation, we show

$$C_2 = \begin{bmatrix} -a_5 & \frac{-a_4(a_2+a_3)}{(a_6+a_7)} & a_4 \\ (a_6+a_7) & -a_8 & 0 \\ 0 & n & -a_1 \end{bmatrix},$$

where $n = \frac{(a_2+a_3)(a_1-a_8)}{(a_6+a_7)}$.

Based on the value of n, we classify two cases.

Case 1. if $n \neq 0$,

Let

$$M_2 = B_4 C_2 B_4^{-1}$$

where

$$B_4 = \begin{bmatrix} (a_2+a_3)(a_1-a_8) & \frac{-(a_2+a_3)(a_1^2-a_8^2)}{(a_6+a_7)} & a_1^2 \\ 0 & \frac{(a_2+a_3)(a_1-a_8)}{(a_6+a_7)} & -a_1 \\ 0 & 0 & 1 \end{bmatrix},$$

is the corresponding standard transform matrix.

Utilizing the similarity transformation criteria, we have that $M_2 = M_1$. Further, we transform (22) into eq. (23)

$$(B_4B_3B_2)A_2^2(B_4B_3B_2)^T + M_2(B_4B_3B_2)Q_2(B_4B_3B_2)^T + (B_4B_3B_2)Q_2(B_4B_3B_2)^T M_2^T = 0. \tag{23}$$

Letting

$$\Phi_2 = \frac{1}{q_2^2}(B_4B_3B_2)Q_2(B_4B_3B_2)^T,\ q_2 = (a_2+a_3)(a_1-a_8)\eta_2.$$

Therefore, (23) becomes

$$A_0^2 + M_2\Phi_2 + \Phi_2 M_2^T = 0.$$

As highlighted in the first Step, Φ_2 is positive definite. Therefore,

$$Q_2 = q_2^2(B_4B_3B_2)^{-1}\Phi_2((B_4B_3B_2)^T)^{-1}.$$

Case 2. if $n = 0$,

Let

$$M_{2n} = B_{4n} C_2 B_{4n}^{-1},$$

where the standard transform matrix

$$B_{4n} = \begin{bmatrix} (a_6+a_7) & -a_8 & 0 \\ 0 & 1 & 0 \\ 0 & 0 & 1 \end{bmatrix},$$

which can be obtained by the method (II) in [29], by the uniqueness of the standard $\mathcal{R}_2$ matrix of M then we obtain

$$M_{2n} = \begin{bmatrix} -\varpi_1 & -\varpi_2 & -\varpi_3 \\ 1 & 0 & 0 \\ 0 & 0 & -a_1 \end{bmatrix}.$$

As the polynomial shown above is similarity invariant, therefore we obtain

$$P_M(r) = r^3 + p_1r^2 + p_2r + p_3 = P_{M_{2n}}(r) = r^3 + (\varpi_1 + a_1)r^2 + (\varpi_2 + \varpi_1 a_1)r + (\varpi_2 a_1).$$

Consequently

$$\begin{aligned} \varpi_1 &= p_1 - a_1 = a_5 + a_8 > 0 \\ \varpi_2 &= p_2 - \varpi_1 a_1 = p_2 - a_1(a_5 + a_8) = a_4(a_2+a_3)a_8a_5 > 0. \end{aligned} \tag{24}$$

In a similar way, we proceed as

$$(B_{4n}B_3B_2)A_1^2(B_{4n}B_3B_2)^T + M_{2n}(B_{4n}B_3B_2)Q_2(B_{4n}B_3B_2)^T + (B_{4n}B_3B_2)Q_2(B_{4n}B_3B_2)^T M_{2n}^T = 0. \tag{25}$$

Letting

$$\bar{\Phi}_2 = \frac{1}{\bar{q}_2^2}(B_{4n}B_3B_2)Q_2(B_{4n}B_3B_2)^T,\quad \bar{q}_2 = (a_6+a_7)\eta_2,$$

algebraic equation (25) becomes

$$A_0^2 + M_{2n}\bar{\Phi}_2 + \bar{\Phi}_2 M_{2n}^T = 0.$$

By Lemma (3) and (24), $\bar{\Phi}_2$ is semi-positive definite, it is given in the following form

$$\bar{\Phi}_2 = diag\left(\frac{1}{2\varpi_1}, \frac{1}{2\varpi_1\varpi_2}, 0\right).$$

Therefore,

$$Q_2 = \bar{q}_2^2(B_{4n}B_3B_2)^{-1}\Phi_2((B_{4n}B_3B_2)^T)^{-1}.$$

Step 3.

For the equation that follows,

$$A_3^2 + MQ_3 + Q_3M^T = 0. \tag{26}$$

Let

$$M_3 = B_5MB_5^{-1},$$

where B_5 is given by

$$B_5 = \begin{bmatrix} 0 & 0 & 1 \\ 1 & 0 & 0 \\ 0 & 1 & 0 \end{bmatrix}.$$

By simple calculation, we find

$$M_3 = \begin{bmatrix} -a_8 & 0 & a_6 + a_7 \\ 0 & -a_1 & -(a_2 + a_3) \\ 0 & a_4 & -a_5 \end{bmatrix}.$$

Further, (26) can be transformed into eq.(27)

$$B_5A_3^2B_5^T + M_3B_5Q_3B_5^T + B_5Q_3B_5^TM_3^T = 0. \tag{27}$$

Letting

$$\Phi_3 = \frac{1}{\eta_3^2}B_5Q_3B_5^T,$$

eq. (27) becomes

$$D_0^2 + M_3\Phi_3 + \Phi_3M_3^T = 0.$$

By Lemma (4), Φ_3 is semi-positive definite, it is given in the following form $\Phi_3 = diag(\frac{1}{2a_8}, 0, 0)$. Thus

$$Q_3 = \eta_3^2B_5^{-1}\Phi_3(B_5^T)^{-1}.$$

Therefore, the real symmetric matrix $Q = Q_1 + Q_2 + Q_3$ in eq. (12) is positive definite, then there is a local and approximately log-normal density function $\varphi(Y)$ near $\mathcal{E}^*$. □

4 Numerical results

In this section, we carry out numerical simulation to illustrate the theoretical results.

4.1 Milstein method

The Milstein method is an approach used to obtain approximate numerical solutions for SDEs. Originally introduced by Grigori N. Milstein in [34], this method offers an effective way to solve SDEs of the form:

$$d\mathfrak{X}(t) = g(t, \mathfrak{X}(t))dt + h(t, \mathfrak{X}(t))dW(t), \qquad \mathfrak{X}(0) = \mathfrak{X}_0. \tag{28}$$

Using the Milstein method as follows:

$$\mathfrak{X}^{n+1} = \mathfrak{X}^n + g(\mathfrak{X}^n, t^n)\Delta t + h(\mathfrak{X}^n, t^n)\Delta W^n + 0.5h(\mathfrak{X}^n, t^n)h'(\mathfrak{X}^n, t^n)((\Delta W^n)^2 - \Delta t), \tag{29}$$

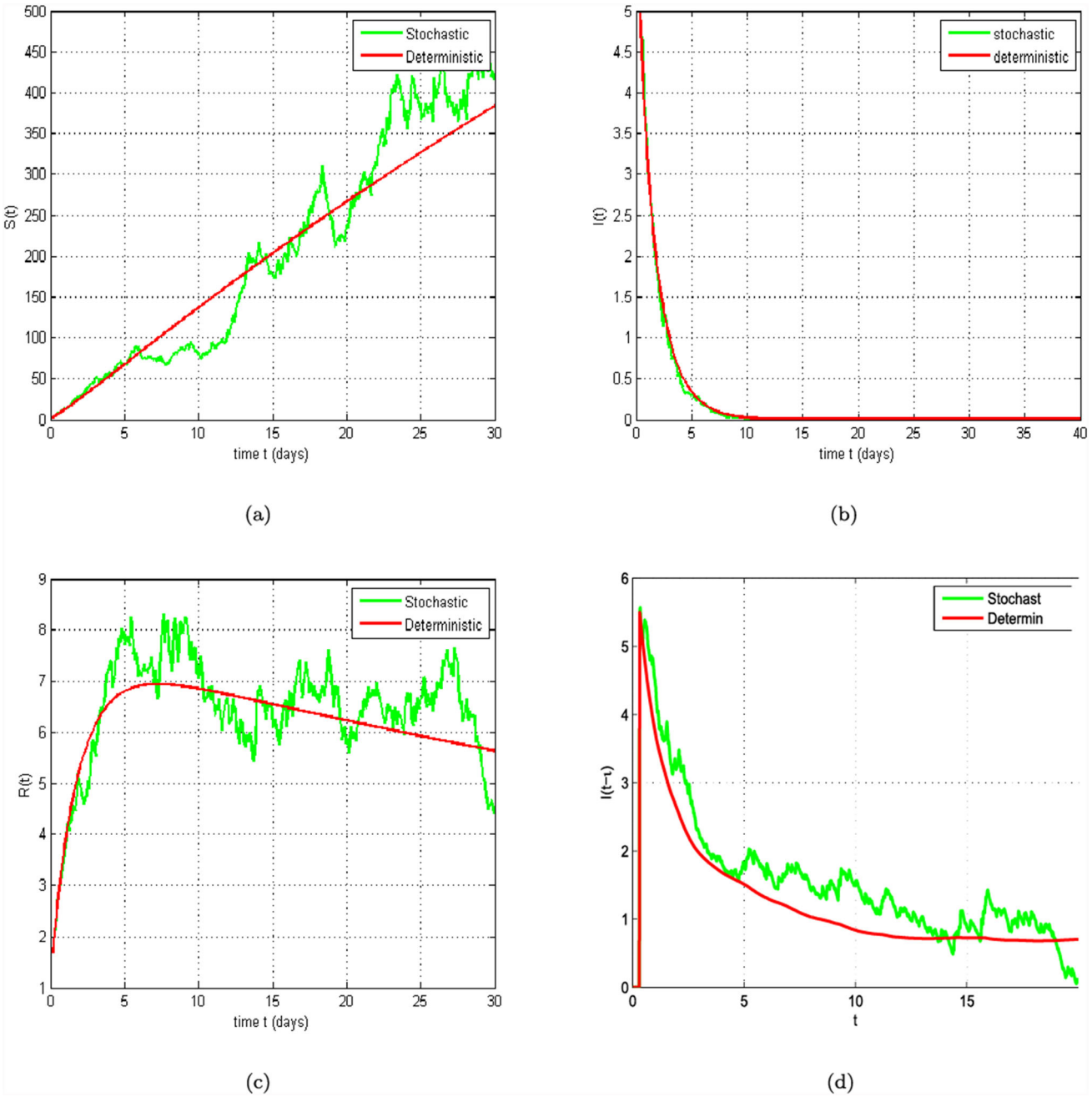

Fig. 1 Computer simulation of the deterministic and stochastic path of solution of model (4) using parameters of example 1

where $h'(x,\ t)$ denotes the derivative of $h(x,\ t)$ w.r.t x and $\Delta W = W(t_{n+1}) - W(t_n)$ is the Brownian increment on $[t_n,\ t_{n+1}]$. Now, we will use this method (29) to solve the system (4) numerically as follows:

$$\begin{aligned}
S^{n+1} &= S^n + \left[\Lambda - \frac{\gamma S^n I^n}{(1+\alpha_1 S^n)(1+\alpha_2 I^n)} - \upsilon S^n + \delta_0 e^{-\upsilon\kappa} I^{n-\kappa}\right]\Delta t + \eta_1 S^n \Delta W^n + 0.5\ \eta_1^2 S^n((\Delta W_1^n)^2 - \Delta t)\\
I^{n+1} &= I^n + \left[\frac{\gamma S^n I^n}{(1+\alpha_1 S^n)(1+\alpha_2 I^n)} - \frac{aI^n}{1+bI^n} - (\upsilon+\delta+\lambda)I^n\right]\Delta t + \eta_2 I^n \Delta W_2^n + 0.5\ \eta_2^2 I^n((\Delta W_2^n)^2 - \Delta t) \qquad (30)\\
R^{n+1} &= R^n + \left[\frac{aI^n}{1+bI^n} - \upsilon R^n + \delta I^n - \delta_0 e^{-\upsilon\kappa} I^{n-\kappa}\right]\Delta t + \eta_3 R^n \Delta W_3^n + 0.5\ \eta_3^2 R^n((\Delta W_3^n)^2 - \Delta t).
\end{aligned}$$

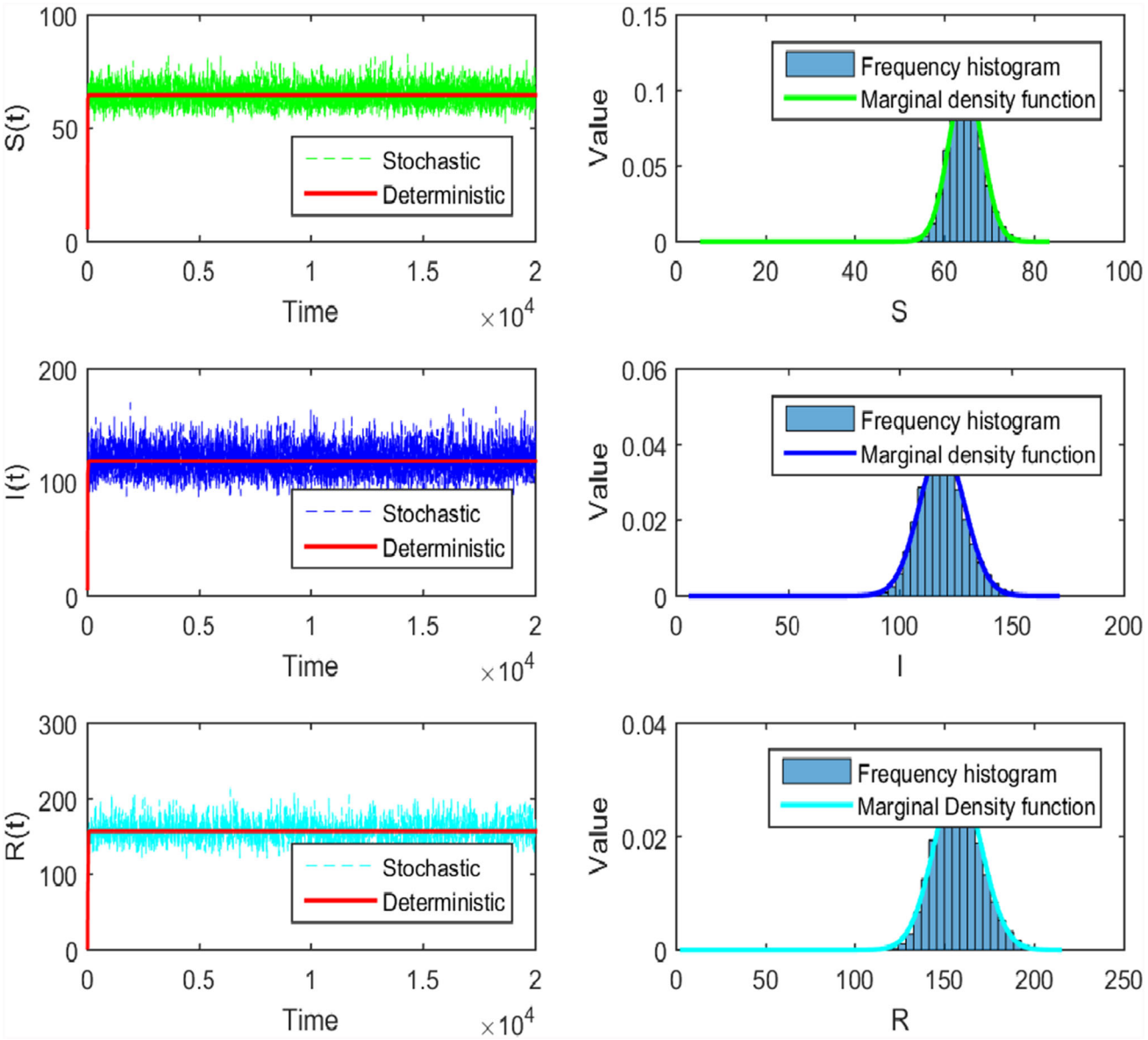

Fig. 2 Compartment S, I, and R in the deterministic and stochastic system are simulated in the left hand column. The frequency histogram and marginal density function graphs for S, I, and R are displayed in the right hand column, using parameters of example 2

Also, the explicit solutions can be written as follows:

$$\begin{aligned}
S^{n+1} &= S^n + \left[\Lambda - \frac{\gamma S^n I^n}{(1+\alpha_1 S^n)(1+\alpha_2 I^n)} - \upsilon S^n + \delta_0 e^{-\upsilon\kappa} I^{n-\kappa}\right]\Delta t + \eta_1 S^n \sqrt{(\Delta t)}\varsigma_1(n) + 0.5\,\eta_1^2 S^n(\sqrt{(\Delta t)}\varsigma_1(n))^2 - \Delta t)\\
I^{n+1} &= I^n + \left[\frac{\gamma S^n I^n}{(1+\alpha_1 S^n)(1+\alpha_2 I^n)} - \frac{aI^n}{1+bI^n} - (\upsilon+\delta+\lambda)I^n\right]\Delta t + \eta_2 I^n \sqrt{(\Delta t)}\varsigma_2(n) + 0.5\,\eta_2^2 I^n((\sqrt{(\Delta t)}\varsigma_2(n))^2 - \Delta t) \quad (31)\\
R^{n+1} &= R^n + \left[\frac{aI^n}{1+bI^n} - \upsilon R^n + \delta I^n - \delta_0 e^{-\upsilon\kappa} I^{n-\kappa}\right]\Delta t + \eta_3 R^n \sqrt{(\Delta t)}\varsigma_3(n) + 0.5\,\eta_3^2 R^n((\sqrt{(\Delta t)}\varsigma_3(n))^2 - \Delta t),
\end{aligned}$$

where $\varsigma_i(n)$, $i = 1, 2, 3,$ represents independent Gaussian random variables with $N(0, 1)$, and Δt shows the increment in time.

4.2 Numerical simulation

The following aspects will be highlighted through a number of empirical examples:

- The dynamical behavior of model (4) if $R_0 < 1$.
- The existence of stationary distribution of (4), and the special expression of the unique density function if $\bar{R}_0 > 1$.

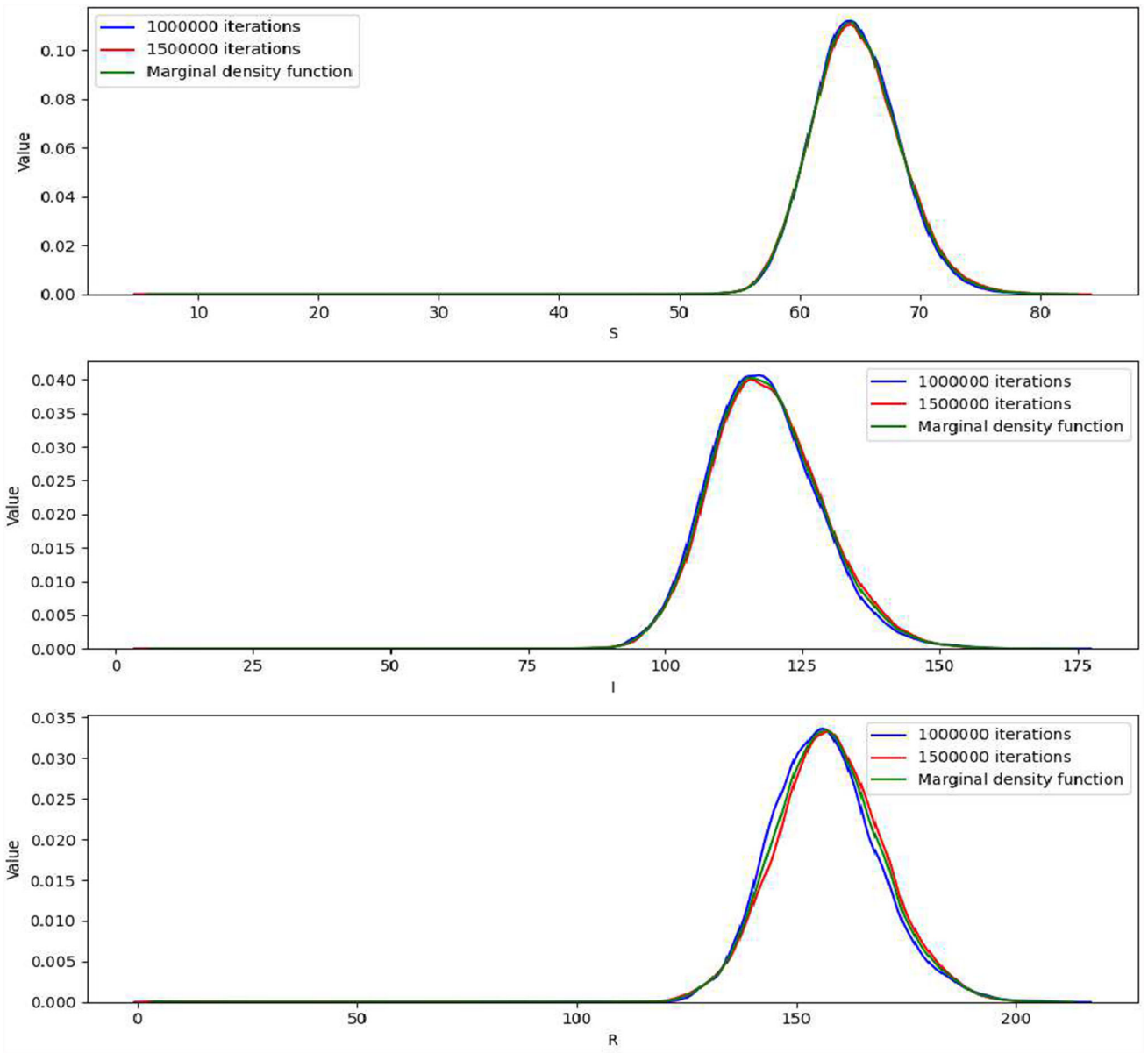

Fig. 3 Computer simulation for S, I, and R, the marginal density curves are represented by the green lines. At 1500000 iteration and 1000000 iteration, the frequency histogram fitting trajectories of S, I, and R represented by the lines red and blue, respectively

- The impact of changing the delay time ι on the epidemic dynamics.
- Effect of saturated treatment rate and Crowley–Martin incidence rate parameters on the epidemic dynamics.

Example 1 To illustrate extinction of disease in the two models: deterministic and stochastic, the following parameters values are assumed (some parameters are taken from [5]): $\Lambda = 15$, $\gamma = 0.014$, $\upsilon = 0.03$, $\iota = 1$, $\eta_1 = 0.12$, $\eta_2 = 0.25$, $\eta_3 = 0.05$, $\alpha_1 = 0.21$, $\alpha_2 = 0.21$, $\delta = 0.25$, $\delta_0 = 0.023$, $a = 0.3$, $b = 0.1$, $\lambda = 0.03$, then $R_0 = 0.1954 < 1$, and $S(0) = 2.5$, $I(0) = 5.5$, $R(0) = 1.7$. (See Fig. 1).

From Fig. 1, we observe that the number of infected people becomes zero over time, which means that the epidemic will become extinct from the population.

Example 2 We choose the following parameters: $\Lambda = 35$, $\gamma = 0.659$, $\upsilon = 0.096$, $\iota = 0$, $\eta_1 = 0.0399$, $\eta_2 = 0.0573$, $\eta_3 = 0.029$, $\alpha_1 = 0.029$, $\alpha_2 = 0.4897$, $\delta = 0.0458$, $\delta_0 = 0.0081$, $a = 0.1$, $b = 0.001$, $\lambda = 0.02$, then $\bar{R}_0 = 25.9318 > 1$, with $S(0) = 5.8$, $I(0) = 6.5$, $R(0) = 3.3$. By theorem (3), the system (4) possesses a unique SD (see left column in Fig. 2). Biologically, this means that the disease will persist in the population and will not be naturally eliminated under the present condition.

By theorem (4), SD around $\mathcal{E}^*$ has unique log-normal density $\varphi(S, I, R)$; in addition, the calculation shows that $(S^*, I^*, R^*) \backsimeq (64.66, 118.43, 156.81)$ and $n = 0.7199 \neq 0$, thus

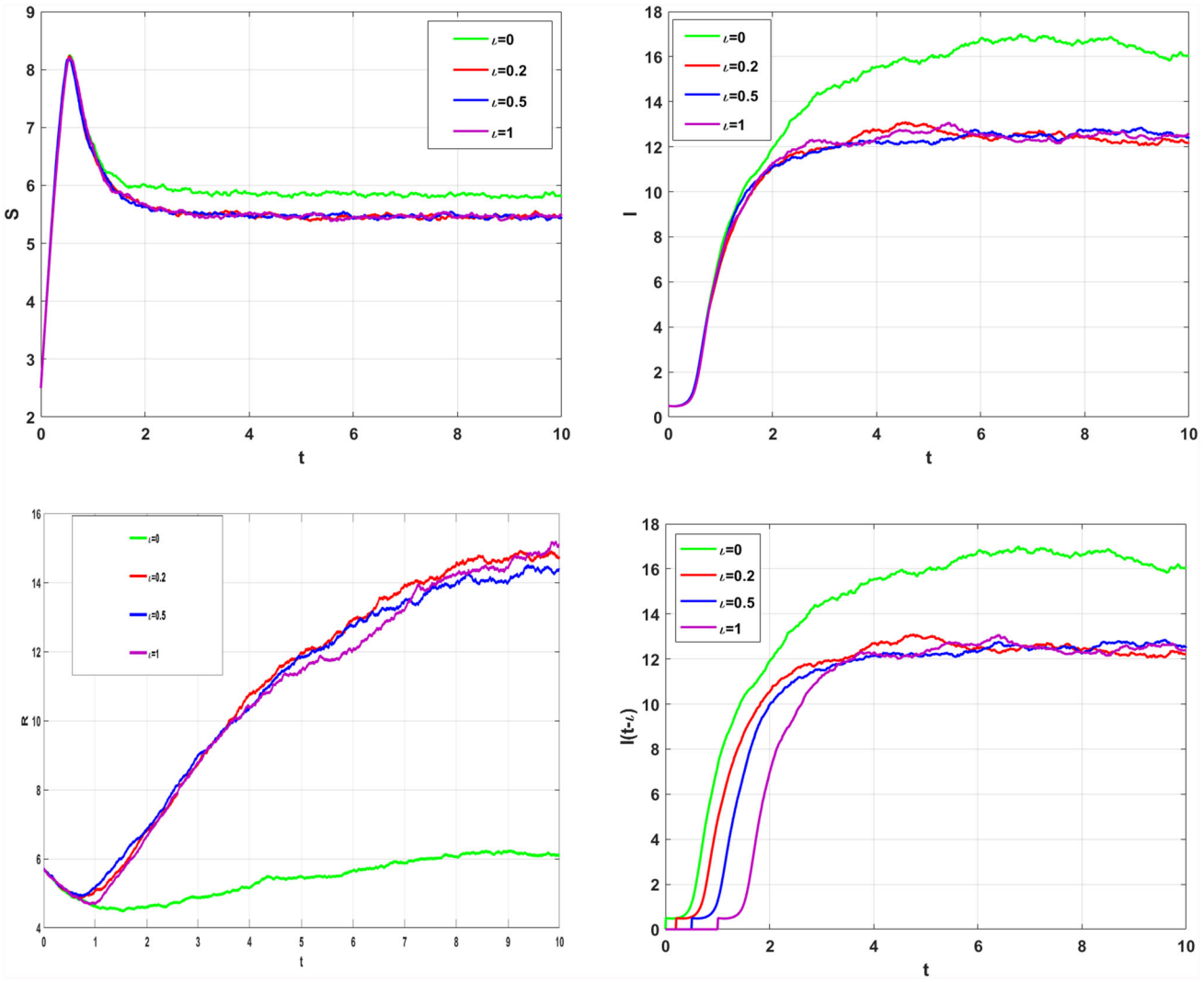

Fig. 4 Computer simulation for solution of model (4) with different values of time delay ι and intensity white noise $\eta_1 = \eta_2 = \eta_3 = 0.02$

$$Q \backsimeq \begin{pmatrix} 0.0125 & -0.0126 & -0.0022 \\ -0.0126 & 0.0130 & 0.0010 \\ -0.0022 & 0.0010 & 0.0051 \end{pmatrix}.$$

The marginal density function of S, I, and R can be determined by the following

$$\frac{\partial \varphi}{\partial S} \rightsquigarrow \mathcal{N}(64.66,\ 0.0125);\ \ \frac{\partial \varphi}{\partial I} \rightsquigarrow \mathcal{N}(118.43,\ 0.0130);\ \ \frac{\partial \varphi}{\partial R} \rightsquigarrow \mathcal{N}(156.81,\ 0.0051)$$

the results can be viewed in Fig. 3, and the right column in Fig. 2 that shows the corresponding density function and frequency histogram.

Example 3 We use the following parameters [5]:$\Lambda = 15, \alpha_1 = 0.1,\ \alpha_2 = 0.1,\ \gamma = 0.2,\ \delta = 0.25, \delta_0 = 0.23,\ \upsilon = 0.3, a = 0.3,$ $b = 1,\ \lambda = 0.4,$ and the following initial conditions: $S(0) = 2.5, I(0) = 0.5, R(0) = 5.7$. Also, we use different values of time delay $\iota,$ and $\eta_1,\ \eta_2,\ \eta_3$. Fig 4, 5, show the solution behavior for the considered model (4) with different values of time delay $\iota,$ and $\eta_1,\ \eta_2,\ \eta_3$.

From our observations, the number of infected individuals is highest when $\iota = 0$ compared to when $\iota = 0.2$,0.5 and 1. This indicates that as the duration of immunity increases, the overall prevalence of infection decreases. The parameter ι represents the duration of immunity, with higher values corresponding to a longer period of immunity following recovery. When immunity is

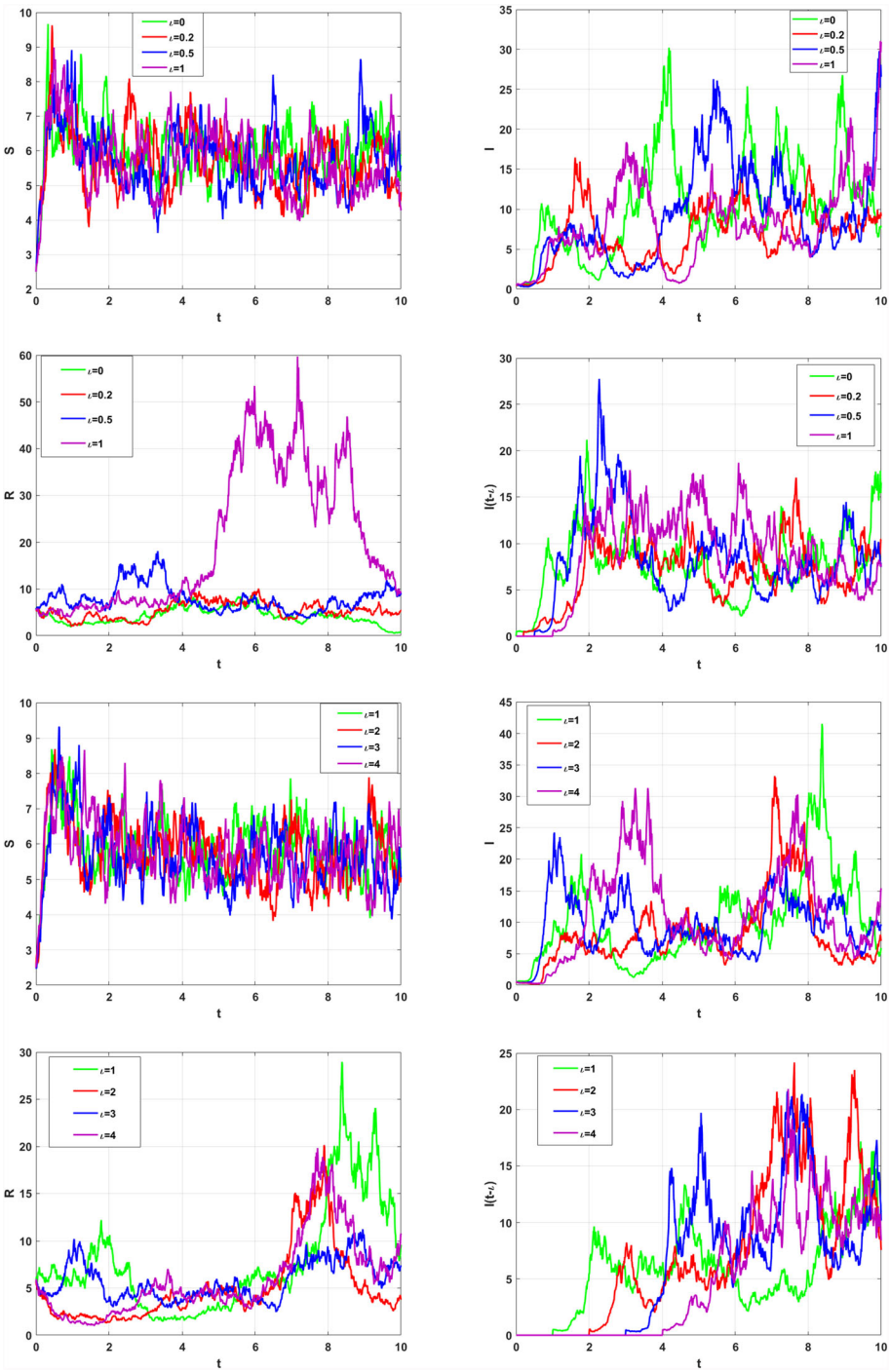

Fig. 5 Computer simulation for solution of model (4) with different values of time delay ι and intensity white noise $\eta_1 = 0.45$, $\eta_2 = 0.65$, $\eta_3 = 0.5$

short-lived, recovered individuals quickly become susceptible again, leading to a higher number of reinfections and a sustained high level of infection in the population. However, as ι increases, recovered individuals remain immune for a longer duration, reducing the pool of susceptible individuals and consequently lowering the rate of new infections. This trend suggests that extending immunity—whether through natural infection, vaccination, or booster doses—can significantly contribute to controlling disease transmission and reducing the burden of infection within a population.

Example 4 In Figs. 6, 7, and 8, the effect of the parameters of saturated treatment rate and Crowley–Martin incidence is shown, by using the parameters of example 1 and example 2.

Fig. 6 displays the impact of cure rate a and treatment availability limitation rate b on infected individuals for different values of a and b and $R_0 < 1$. The right side of Fig. 6 shows that increasing cure rate a leads to a decrease in the number of infected

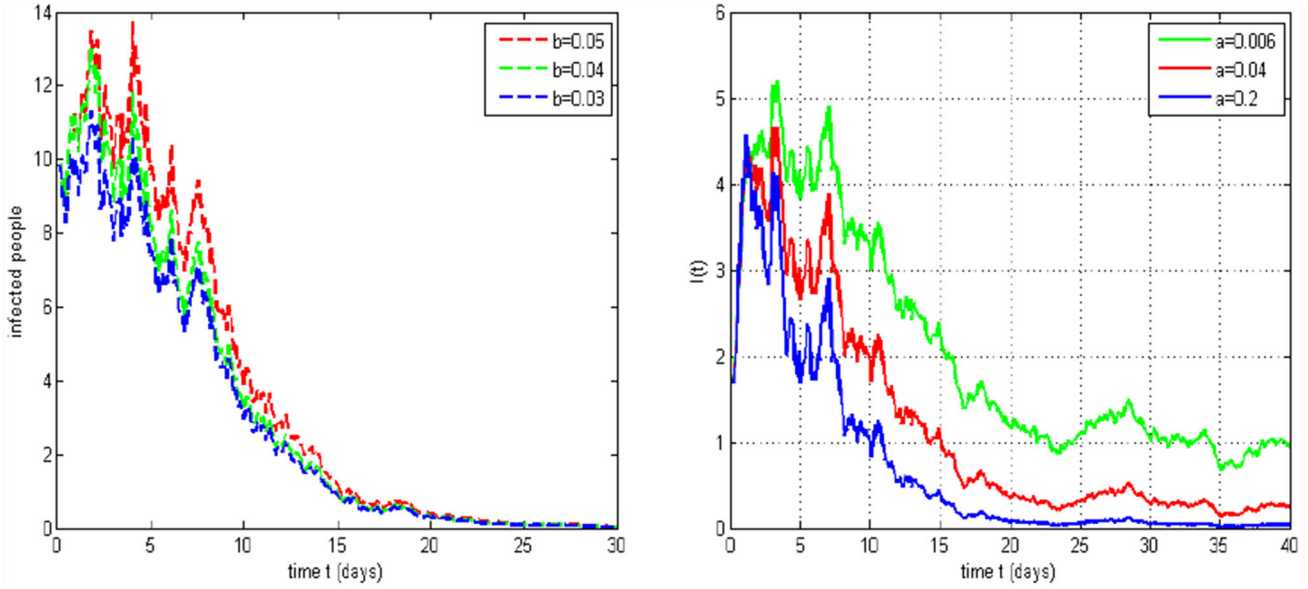

Fig. 6 Computer simulations for the numbers of infected people of model (4) with different HT-II treatment rate parameters a and b

Fig. 7 Computer simulation for the number of infected people with and without HT-II treatment rate

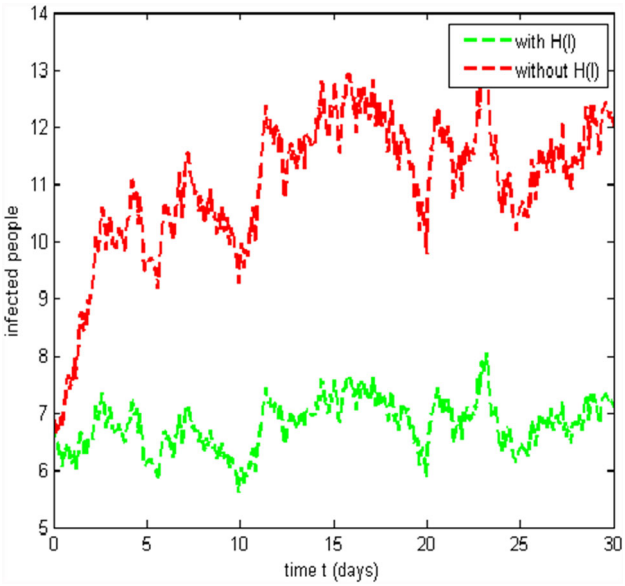

individuals. The left side of Fig. 6 shows that with an increase in the value of b an increase in the number of infected population is due to the limited resources in the community.

The difference in the infected population at with and without treatment rate $H(I)$ is depicted in Fig. 7. It is evident that if HT-II treatment is administered to the sick population will substantially decrease the number of infected individuals.

The infected population at different values of α_1 and α_2 is depicted in Fig. 8. It is evident that an increase in α_1 and α_2 corresponds with a decrease in the infected population. It demonstrates that greater values of α_1 and α_2, respectively, will prevent the illness from spreading. Therefore, it may be said that susceptible and infectious individuals who adopt preventive actions will help to slow the spread of illness.

Through the integration of theoretical analysis and numerical simulations, we discovered that smaller white noise enables model (4) to exhibit a unique ergodic **SD** when $\bar{R}_0 > 1$. Conversely, larger white noise can lead to disease extinction in model (4) when $R_0 < 1$. In comparison with the deterministic model, the inclusion of random white noise and time delay in the epidemic model significantly influences the persistence and extinction of the disease, thereby enriching the dynamic behavior of the epidemic model.

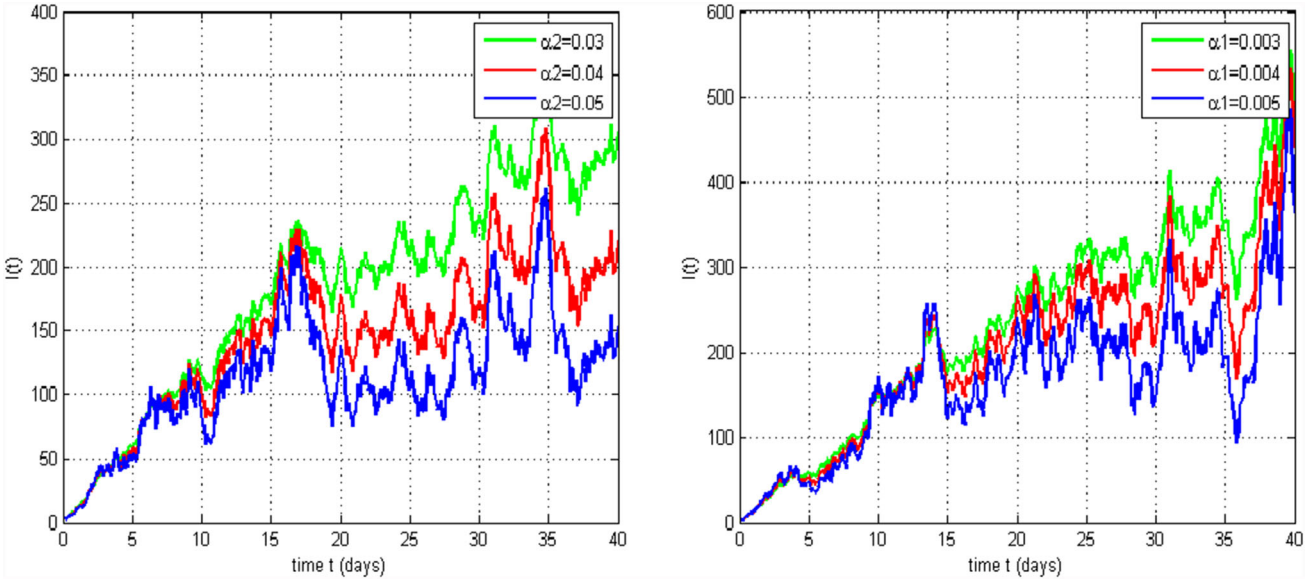

Fig. 8 Computer simulations for the numbers of infected people of model (4) with different C−M rate parameters α_1 and α_2

5 Conclusion

This study has thoroughly explored a time-delayed stochastic *SIR* model that incorporates HT−II treatment and Crowley–Martin incidence, allowing us to investigate the dynamics of disease spread under realistic conditions. By rigorously establishing the stability, uniqueness, and existence of solutions, we provide a solid theoretical foundation for understanding the behavior of the model over time. This framework ensures that the model maintains biological consistency, which is essential for making reliable predictions about epidemic outcomes. We further identified the critical parameters that govern disease extinction and highlighted the roles of various factors, including transmission rates, treatment effectiveness, and time delays, which can influence whether an epidemic is eradicated. The probability density function is analytically derived, offering a deeper insight into the model's stochastic behavior, particularly near the endemic equilibrium. This analytical formulation is crucial for evaluating the likelihood of disease persistence and predicting potential fluctuations in infection rates. Further to this, the theoretical results were rigorously verified through a comprehensive numerical simulation. The simulation underscores the significant impact of nonlinear incidence and treatment rates as well as the role of temporal delays on the dynamics and control of the disease. Furthermore, the numerical experiments highlight the importance of both deterministic and stochastic effects for accurate modeling of real-world disease transmission. In conclusion, this study not only advances our theoretical understanding of epidemic dynamics under time delays and stochastic influences but also offers practical tools for improving epidemic forecasting and intervention planning. The incorporation of more realistic epidemiological assumptions into the modeling efforts represents an important step toward more robust and reliable predictions, ultimately aiding in the global effort to control infectious diseases. Moreover, we believe this study helps in providing public health interventions, serving as a foundation for targeted strategies to minimize disease incidence and prevent future outbreaks.

Acknowledgements The authors extend their appreciation to the Deanship of Research and Graduate Studies at King Khalid University, KSA for funding this work through Large Research Project under grant number RGP.2/63/45. This research also received financial support from the European Union under the REFRESH—Research Excellence for Regional Sustainability and High-Tech Industries project, number CZ.10.03.01/00/22_003/0000048, through the Operational Programme Just Transition.

Data availability The authors confirm that no data has been used in this study.

Declarations

Conflict of interest There is no conflict of interest among the authors.

References

1. Q.T. Ain, Nonlinear stochastic cholera epidemic model under the influence of noise. J Math Tech Model **1**(1), 52–74 (2024)
2. S.M.A. Shah, H. Tahir, A. Khan, A. Arshad et al., Stochastic model on the transmission of worms in wireless sensor network. J Math Tech Model **1**(1), 76–89 (2024)
3. W.O. Kermack, A.G.M. McKendrick, A contribution to the mathematical theory of epidemics. Proc. R. Soc. Lond. A **115**, 70021 (1927)

4. A. Kumar, Nilam, Stability of a time delayed SIR epidemic model along with nonlinear incidence rate and holling type-ii treatment rate. Int. J. Comput. Methods **15**(6), 1850055 (2018)
5. Xiaoyun Zhonga, Shangjiang Guoa, Minfang Pengb, Stability of stochastic SIRS epidemic models with saturated incidence rates and delay. Stoch Anal Appl **35**(1), 1–26 (2017)
6. A. Din, Y. Li, A. Yusuf, Delayed hepatitis B epidemic model with stochastic analysis. Chaos, Solitons & Fractals **146**, 110839 (2021)
7. Dan Li, Fengying Wei, Xuerong Mao, SD and density function of a stochastic SVIR epidemic model. J. Franklin Inst. **359**(16), 9422–9449 (2022)
8. B. Dubey, A. Patara, P.K. Srivastava, U.S. Dubey, Modelling and analysis of a SEIR model with different types of nonlinear treatment rates. J. Biol. Syst. **21**(3), 1350023 (2013)
9. Z. Liu, Dynamics of positive solutions to SIR and SEIR epidemic models with saturated incidence rates. Nonlinear Anal: Real World Appl **14**(3), 1286–1299 (2013)
10. F.A. Rihan, H.J. Alsakaji, C. Rajivganthi, Stochastic SIRC epidemic model with time-delay for COVID-19. Adv Differ Equ **2020**(1), 502 (2020)
11. M.A. Khan, M. Ismail, S. Ullah, M. Farhan, Fractional order SIR model with generalized incidence rate. AIMS Math **5**(3), 1856–1880 (2020)
12. A. Din, Bifurcation analysis of a delayed stochastic HBV epidemic model: cell-to-cell transmission. Chaos, Solitons & Fractals **181**, 114714 (2024)
13. E. Tornatore, S.M. Buccellato, P. Vetro, stability of stochastic SIR system. Phys. A **354**, 111–126 (2005)
14. W. Wang, S. Ruan, Bifurcation in an epidemic model with constant removal rates of the infective. J. Math. Anal. Appl. **21**, 775793 (2004)
15. X. Zhang, X. Liu, Backward bifurcation of an epidemic model with saturated treatment function. J. Math. Anal. Appl. **348**, 433443 (2008)
16. Mahmood Parsamanesh, Majid Erfanian, Global dynamics of an epidemic model with standard incidence rate and vaccination strategy. Chaos, Solitons & Fractals **117**, 192–199 (2018)
17. W. Zhao, J. Liu, M. Chi et al., Dynamics analysis of stochastic epidemic models with standard incidence. Adv Differ Equ **2019**(1), 1–16 (2019)
18. V. Capasso, G. Serio, A generalization of the Kermack McKendrick deterministic epidemic model. Math. Biosci. **42**(1), 4361 (1978)
19. A. Kumar, Dynamic behavior of an SIR epidemic model along with time delay; CrowleyMartin type incidence rate. Int J Nonlinear Sci Numer Simul **20**(7–8), 757–771 (2019)
20. Milica Milunovi, Marija Krsti, Long time behavior of an two diffusion stochastic SIR epidemic model with nonlinear incidence and treatment. Filomat **36**(8), 28292846 (2022)
21. M. El Fatini, I. Sekkak, R. Taki, T. El Guendouz, A control treatment for a stochastic epidemic model with relapse and Crowly-Martin incidence. J Anal **29**, 713–729 (2021)
22. P.H. Crowly, E.K. Martin, Functional responses and interference within and between year classes of a dragonfly population. J. North Am. Benth. Soc. **8**, 211221 (1989)
23. P. Dubey, B. Dubey, U.S. Dubey, An SIR model with nonlinear incidence rate and Holling type III treatment rate. Appl. Anal. Biol. Phys. Sci. **186**, 6381 (2016)
24. L. Wen, X. Yang, Global stability of a delayed SIRS model with temporary immunity. Chaos Soliton Fract. **38**, 221226 (2008)
25. R. Xu, Z. Ma, Z. Wang, Global stability of a delayed SIRS epidemic model with saturation incidence and temporary immunity. Comput. Math. Appl. **59**, 32113221 (2010)
26. Y.N. Kyrychko, K.B. Blyuss, Global properties of a delayed SIR model with temporary immunity and nonlinear incidence rate. Nonlinear anal real world Appl **6**(3), 495–507 (2005)
27. Y. Zhao, D. Jiang, D. O'Regan, The extinction and persistence of the stochastic SIS epidemic model with vaccination. Phys. A **392**, 49164927 (2013)
28. X. Wang, A simple proof of descartess rule of signs. Am. Math. Mon. (2004). https://doi.org/10.2307/4145072
29. B. Zhou, X. Zhang, D. Jiang, Dynamics and density function analysis of a stochastic SVI epidemic model with half saturated incidence rate. Chaos Soliton Fractals **137**, 109865 (2020)
30. B. Zhou, D. Jiang, Y. Dai, T. Hayat, A. Alsaedi, SD and PDF of a stochastic SVIS epidemic model with standard incidence and vaccination strategies. Chaos, Solitons Fractals **143**, 110601 (2021)
31. C.W. Gardiner, *Handbook of stochastic methods for physics chemistry and the natural sciences* (Springer, Berlin, 1983)
32. H. Roozen, An asymptotic solution to a two-dimensional exit problem arising in population dynamics. SIAM J. Appl. Math. **49**, 1793 (1989)
33. X. Tian, C. Ren, Linear equations, superposition principle and complex exponential notation. Coll Phys **23**, 235 (2004)
34. G.N. Mil'shtein, Approximate integration of stochastic differential equations. Teoriya Veroyatnostei i ee Primeneniya (in Russian) **19**(3), 583–588 (1974)